CHALMERS
UNIVERSITY OF TECHNOLOGY

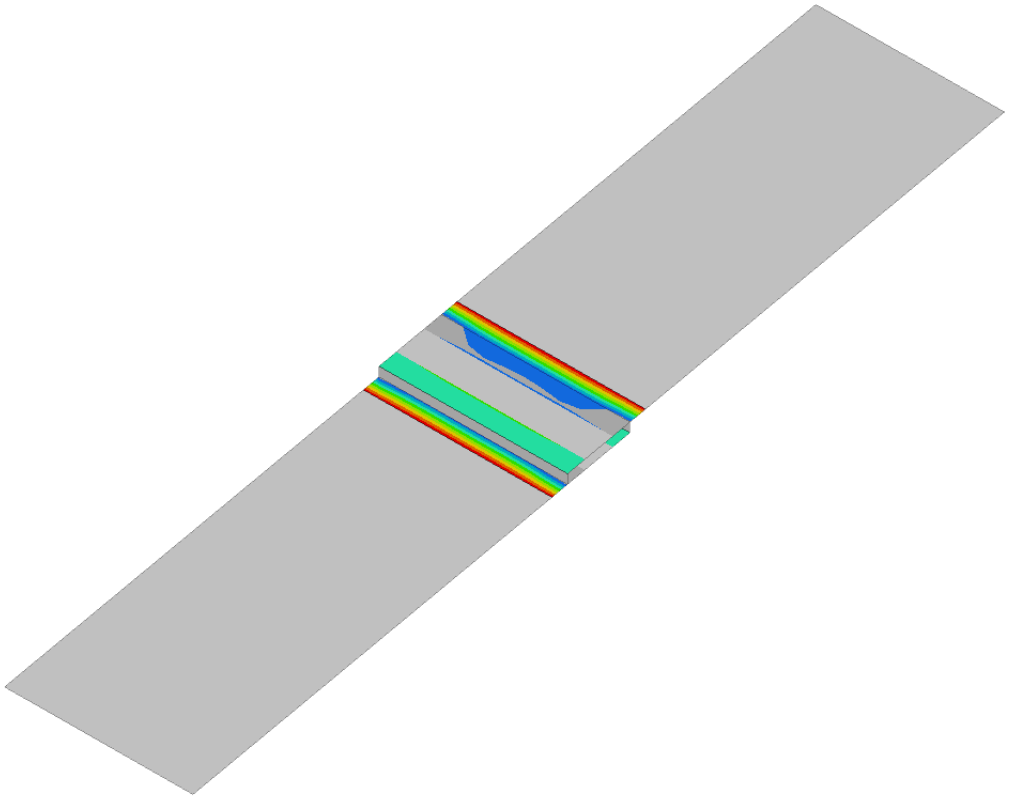

Fatigue Life Prediction in Aluminium Welds for Thin-sheet Structures

Master's thesis in Applied Mechanics

ROBIN KRISTIANSSON
FILIP NORBERG

DEPARTMENT OF MECHANICS AND MARITIME SCIENCES

CHALMERS UNIVERSITY OF TECHNOLOGY
Gothenburg, Sweden 2022
www.chalmers.se

Master's thesis 2022

Fatigue Life Prediction in Aluminium Welds for Thin-sheet Structures

ROBIN KRISTIANSSON

FILIP NORBERG

CHALMERS
UNIVERSITY OF TECHNOLOGY

Department of Mechanics and Maritime Sciences
Division of Dynamics
Chalmers University of Technology
Gothenburg, Sweden 2022

Fatigue Life Prediction in Aluminium Welds for Thin-sheet Structures
ROBIN KRISTIANSSON
FILIP NORBERG

Supervisor: CAE Engineer, Mikael Hanneberg, AFRY
Examiner: Prof. Anders Ekberg, Mechanics and Maritime Sciences

Master's Thesis 2022:45
Department of Mechanics and Maritime Sciences
Division of Dynamics
Chalmers University of Technology
SE-412 96 Gothenburg
Telephone +46 31 772 1000

Cover: Finite Element Model of a welded lap joint, simulated in OptiStruct and visualized in HyperView.

Typeset in LaTeX
Printed by Chalmers Reproservice
Gothenburg, Sweden 2022

Fatigue Life Prediction in Aluminium Welds for Thin-sheet Structures
ROBIN KRISTIANSSON
FILIP NORBERG
Department of Mechanics and Maritime Sciences
Chalmers University of Technology

Abstract

Current codes and recommendations used for fatigue analysis of welded joints are mainly developed for the civil and maritime sectors where the material thickness used is typically more than 5 mm. This is a problem when studying welded components in the automotive industry where the general structure is thinner. This thesis aims to propose and compare two methods with different level of modelling detail developed for thin-walled structures with a material thickness of less than 5 mm. The methods proposed are found from a study of relevant research and are implemented on two different joints. A series of different load cases were simulated and a comparison of the results was made with the aim of finding any discrepancies between the methods, both concerning fatigue resistance data and stress extraction. The findings suggests that the major deviation between the methods is related to the fatigue resistance data which is determined from different experimental sources. More interesting was the difference between the methods related to the stress extraction where the deviation in the results depends on the ratio between membrane and bending stresses in the welded joints.

Keywords: welds, fatigue, thin-walled structures, aluminium, FEA, Volvo method, notch stress method

Acknowledgements

This master's thesis was done at the CAE and Safety group at AFRY Trollhättan in collaboration with an U.S. based vehicle developer. The thesis was part of the final project in the master's programme Applied Mechanics at Chalmers University of Technology, Gothenburg, during the spring of 2022.

The authors would like to thank the examiner Professor Anders Ekberg for the guidance in the project. Thanks also to Professor Lennart Josefson for the inputs, enthusiasm and expertise within fatigue and welds. Finally, the authors would like to thank the supervisor Mikael Hanneberg for the support and the other co-workers at AFRY for providing a pleasant working environment.

Gothenburg, June 2022
Filip Norberg and Robin Kristiansson

List of Acronyms

2D	Two-dimensional
CQUAD4	First order quadrilateral shell element in OptiStruct
CTRIA3	First order triangular shell element in OptiStruct
EC9	Eurocode 9
FAT class	Weld fatigue resistance classification
FE	Finite element
FEA	Finite element analysis
FEM	Finite element method
HAZ	Heat-affected zone
HCF	High cycle fatigue
IIW	International Institute of Welding
LCF	Low cycle fatigue
MAG	Metal active gas
RBE2	Rigid body elements
RFC	Rainflow-counting
S-N	Stress-life
SPC	Single-point constraints

Nomenclature

Indices

bot	Index for bottom surface
eq	Index for equivalent
j	Index for load history counting
nC	Index for nCode solver
OS	Index for OptiStruct solver
top	Index for top surface
$\mathrm{x}, \mathrm{y}, \mathrm{z}$	Indices for local directions
$\mathrm{X}, \mathrm{Y}, \mathrm{Z}$	Indices for global directions

Parameters

a	Theoretical weld throat
b	Fatigue strength exponent
D	Damage
e	Plate offset
f	Axial line force
FAT	Fatigue strength coefficient at $N_\mathrm{f} = 2 \cdot 10^6$
k_m	Stress magnification factor
l	Element length
l_f	Free length between supports
l_w	Weld length
m	Line moment
M	Nodal moment
n	Number of cycles with unique stress range
N	Nodal force

N_f	Number of cycles to failure
N_s	Number of sequences to failure
r	Notch radius
R	Stress ratio
s	Support factor
t	Thickness
β	Bending ratio
$\overline{\beta}$	Average bending ratio
β_c	Critical bending ratio
$\Delta\sigma$	Stress range
θ	Weld angle
λ	Factor dependent on degree of restraint
ρ	Actual notch radius
ρ^*	Substitute micro-structural length
ρ_f	Fictitious notch radius
$\sigma_\perp$	Structural stress perpendicular to weld line
σ_1	First principal stress
σ_a	Stress amplitude
σ_b	Bending stress
σ'_f	Fatigue strength coefficient
σ_m	Mean stress
σ_max	Maximum stress
σ_min	Minimum stress
σ_n	Membrane stress
σ_nl	Nonlinear stress
σ_nom	Nominal stress
σ_s	Structural stress
σ_tot	Actual stress states over the thickness at the notch
ϕ_p	Principal stress orientation
ω	Opening angle of the notch

Contents

List of Figures

List of Tables

1

Introduction

The use of aluminium is becoming increasingly common in the automotive industry due to its beneficial strength-to-weight ratio. Since aluminium parts are becoming more common in the vehicles, so do aluminium welds [1]. Being able to understand the effects that the welded joints impose on the structure and how the welding procedure affect the fatigue life of the weld compared to the parent material is crucial to accurately describe the performance of the entire structure. When dealing with fatigue, small errors in the stress and strength are amplified in life predictions and the results become unreliable. This is due to the logarithmic relation between stress and life.

Welds are a versatile joint type for connections that are too complex for forming methods and where the continuation of the joint cross section is beneficial. There are also difficulties that come with welding, such as irregularity of the weld, heat-affected zone (HAZ), residual stresses, distortions, inclusions and stress concentrations in both the weld toe and weld root [2], see geometrical interpretation in Figure 1.1. The residual stresses and weld defects that cause stress concentrations, in combination with cyclic loading will result in early crack initiation and may lead to fatigue failure [2]. Due to the complexity of the weld geometry and the problems surrounding welding, finite element (FE) modelling and fatigue simulations of the welds become difficult. Highly detailed weld geometry models do not always result in better life predictions since they often results in nonphysical stress singularities. One way to avoid numerical errors is to study the global behaviour of the weld and to verify with testing [3].

To overcome the problems discussed, standards and design codes have been developed such as the International Institute of Welding (IIW) recommendations [4] and Eurocode 9 (EC9) [5]. These standards, engineering codes and recommendations can be implemented to study specific problems. Some of the established methods recommended for fatigue prediction from the IIW are the nominal stress method, the hot-spot method and the effective notch method [4]. These methods are aimed at producing stress measures feasible for fatigue life estimations by different analysis methods and with varying levels of detail.

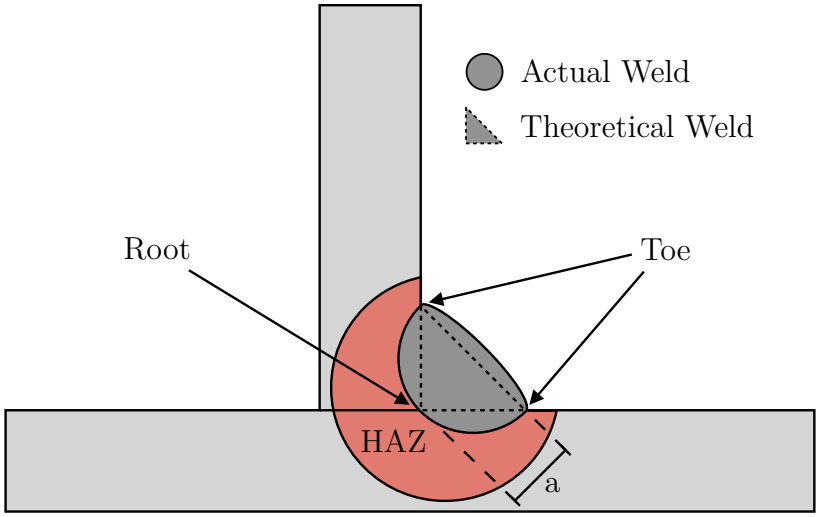

Figure 1.1: Geometrical representation of a one sided fillet weld, showing the differences between the actual and theoretical weld.

The methods have advantages and disadvantages:

- The nominal stress method requires that the joint configuration can be found in recommendations or codes, and that the nominal stress ranges can be determined. This can be difficult in complex structures [6].
- The hot-spot method is mesh and joint dependent but can handle multi-weld fatigue assessment.
- The effective notch method requires a detailed FE model not suitable for models with multiple joints due to computational limitations.
- The fatigue strength reference curves are not specified for specific parent materials or grades, hence the fatigue life estimation will be independent of the mechanical properties of these materials [7].

The methods described in the IIW recommendations were first developed for structures with a thickness between 5 and 25 mm and fatigue assessment of individual welds. This is a problem within the automotive industry since the structure in general is thinner. The notch stress approach was further developed for thin-sheet structures but the proposed approach has not yet been included in the recommendations. To overcome the single weld fatigue assessment, a FE based structural stress method was developed at Chalmers in cooperation with Volvo Cars in the late 1990s. The introduced method can be used for multi-weld fatigue assessment, is more time efficient and can provide sufficiently accurate results [8].

1.1 Problem description

Currently there are no available standards or established recommendations in the automotive industry regarding fatigue assessment of welded structures with thickness below 5 mm. Hence methods and targets for fatigue durability is dependent on each manufacturer [9]. Since the methods proposed for thin-walled structures are not included in any standards or recommendations, questions about the accuracy have been raised. In this thesis the structural stress approach with the Volvo method and the notch stress method for thin-walled structures will be further investigated to examine sensitivities and differences between the methods.

1.2 Objective

The objective of the thesis is to investigate two methods with different level of modelling detail to be used for predicting the fatigue life of thin-walled aluminium welded joints under dynamic loading. The methods should be implemented using the finite element method (FEM) and a comparison between the methods and the nominal stress method from the IIW recommendations should be made.

1.3 Method

To evaluate the results from the Volvo method a comparison will be made with the nominal stress method and notch stress approach. For the nominal stress method the calculation procedures will be implemented in Python 3.9 [10]. For the notch stress approach and the Volvo method the geometrical modelling will take place in CATIA V5-6R2019 [11] and pre-processing in ANSA v21 [12]. Altair OptiStruct 2021 [13] will be used as solver and post-processing for the notch stress approach and Volvo method will be done with a combination of Python 3.9 and META v21 [14].

1.4 Scope and delimitation

This thesis will study two standalone aluminium joints with FEM. The joints should be common in vehicles and have defined FAT classes in the IIW recommendations. Bellow follows a list of topics that will not be included in the scope of this thesis.

- Low cycle fatigue (LCF) will not be considered.
- Residual stresses will not be taken in to account in the elastic analyses but are included in the weld fatigue resistance classification (FAT class).
- Thickness and mean stress correction will not be considered.
- Experimental testing will not be performed and thus the stress-life (S-N) curves need to be validated before operational implementation.

2

Theory

The theoretical framework related to the study is presented in this chapter. General fatigue theory followed by fatigue assessment in welded components are covered. Both analytical and numerical approaches are discussed. Basic knowledge of FEM and fatigue and fracture is expected of the reader. A detailed overview of the fatigue and fracture theory can be found in Dowling [3].

2.1 Fatigue

In contrast to static failure where the failure comes from overloading the materials ultimate strength, fatigue is caused by cyclic loading that leads to crack initiation, propagation and final failure. The fatigue life of a component depends on factors such as the geometry, material, surface finish and stress levels. There are three common methods for studying fatigue, stress-based approaches, strain-based approaches and the fracture mechanics approach. The methods discussed in the thesis are stress-based approaches used for high cycle fatigue (HCF). HCF studies fatigue problems where the response is dominated by elastic behaviour, the stresses are usually below the materials yield strength and the number of cycles to failure N_f is typically above 10^3 [3]. For $N_\mathrm{f} < 10^3$ LCF approaches are used for life prediction. Here strain-based approaches are advantageous since the response commonly is dominated by plastic yielding.

To study the fatigue behaviour of a component, weld or parent material, fatigue testing is essential. This is due to the empirical nature of the fatigue prediction methods. Common in fatigue testing is the use of constant amplitude loading, see Figure 2.1, where the stress varies between maximum stress σ_max and minimum stress σ_min [3]. Using constant amplitude loading, the number of cycles to failure can be determined for different stress levels such that the proper material constants can be fitted to the test data.

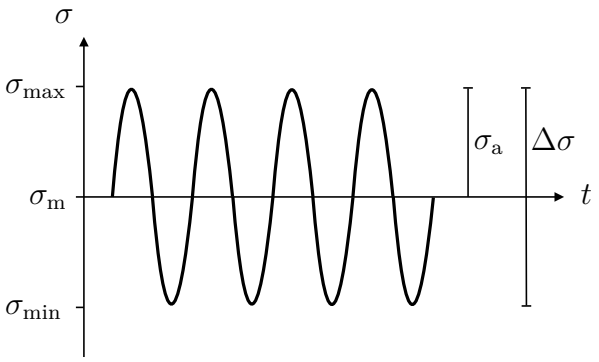

Figure 2.1: Stress sequence of constant amplitude loading.

The stress amplitude σ_a is the variation of the load around the mean stress σ_m. The stress range $\Delta\sigma$ is the difference between σ_max and σ_min. The stress ratio R is the ratio between σ_max and σ_min. The described relations are shown here

$$\sigma_\mathrm{a} = \frac{\sigma_\mathrm{max} - \sigma_\mathrm{min}}{2} \tag{2.1}$$

$$\sigma_\mathrm{m} = \frac{\sigma_\mathrm{max} + \sigma_\mathrm{min}}{2} \tag{2.2}$$

$$\Delta\sigma = \sigma_\mathrm{max} - \sigma_\mathrm{min} \tag{2.3}$$

$$R = \frac{\sigma_\mathrm{min}}{\sigma_\mathrm{max}} \tag{2.4}$$

To conduct fatigue prediction the predominant method for stress-based approaches is the use of S-N curves, also known as Wöhler curves, which describes the predicted relation between the stress and the number of cycles to failure. The S-N curves are determined by extensive testing at various stress levels. The S-N curve is commonly linear in a log-log diagram for HCF, see Figure 2.2. This which is also the assumption made in welding fatigue. The number of cycles to failure at which the knee or fatigue limit of the S-N curve is defined, depends on assumptions made in the method used.

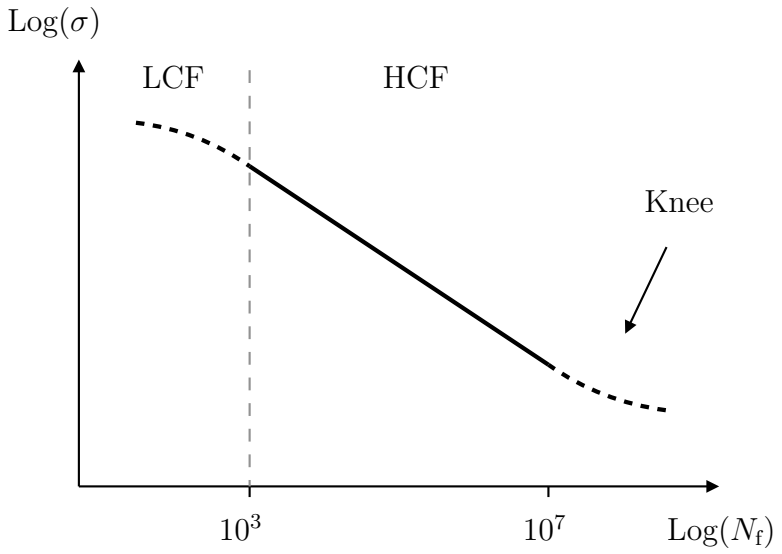

Figure 2.2: Generic S-N curve.

The life in the linear region can be computed by the use of the Basquin equation

$$\sigma_{\mathrm{a}} = \sigma'_{\mathrm{f}} \left(2N_{\mathrm{f}}\right)^{-1/b} \tag{2.5}$$

which is a power law that gives the linear relation in log-log between σ_{a} and N_{f}. The fatigue strength coefficient σ'_{f} and the fatigue strength exponent b are used to fit the curve to test data [3]. For weld fatigue, S-N curves are of the form

$$\Delta\sigma = FAT \left(\frac{N_{\mathrm{f}}}{2 \cdot 10^6}\right)^{-1/b} \text{ or } N_{\mathrm{f}} = 2 \cdot 10^6 \left(\frac{FAT}{\Delta\sigma}\right)^{b} \tag{2.6}$$

where $\Delta\sigma$ is used instead of σ_{a}. The weld fatigue resistance, FAT, is defined as the fatigue strength coefficient at $N_{\mathrm{f}} = 2 \cdot 10^6$ and depends on the method used for fatigue evaluation. The fatigue strength exponent depends on the load type: membrane, bending or shear, the plate thickness of the structure and the fatigue assessment method. In general, for welding fatigue the S-N curve is not dependent on material grade since the fatigue life of welded joints is mainly dependent on the crack growth characteristics. Furthermore, since the crack growth characteristics are usually insensitive to specific alloy and heat treatment the fatigue performance is similar [15], [16].

To study practical problems where load cycles are usually of varying amplitudes, see Figure 2.3, rainflow-counting (RFC) is implemented. RFC is a cycle counting algorithm that outputs $\Delta\sigma$, σ_{m} and the number of cycles n_j corresponding to each unique $\Delta\sigma$.

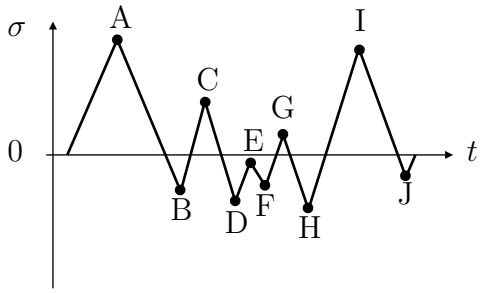

Peaks: A, C, E, G, I

Valleys: B, D, F, H, J

Simple ranges: A-B, B-C, C-D, ..., I-J

RFC ranges: B-C, E-F, D-G, I-J, A-H

Figure 2.3: Stress sequence of variable amplitude load. Adapted from [3].

To compute the life from evaluated stress histories, Palmgren–Miner's cumulative damage rule is used to sum up the total damage

$$D = \frac{n_1}{N_{\mathrm{f},1}} + \frac{n_2}{N_{\mathrm{f},2}} + \frac{n_3}{N_{\mathrm{f},3}} + \cdots + \frac{n_k}{N_{\mathrm{f},k}} = \sum_{j=1}^{k} \frac{n_j}{N_{\mathrm{f},j}} \tag{2.7}$$

where n_j is the number of cycles with unique stress range and amplitude, $N_{\mathrm{f},j}$ is the number of cycles to failure at corresponding stress level and k is the number of stress levels. The number of load sequences to failure is derived from the inverse of the total damage of the sequence (D^{-1}).

2.2 Welds and fatigue

In general, for a component, fatigue estimation is based on the fatigue strength of the parent material and the stress field of the component. For welds the actual stress state is difficult to determine due to the complexity arising from geometrical variations, residual stresses and weld defects. From the welding process the material properties are affected in the vicinity of the weld, the HAZ, and residual stresses are induced. To overcome the problem of predicting the fatigue resistance and stress field, assessment methods based on destructive testing have been developed. The methods were first developed for steel joints with a thickness above 5 mm for railway and bridge applications [17]. Later, some of the engineering codes have included aluminium joints and other applications in the fatigue assessment [4], [5]. The nominal stress method and effective notch stress method are two of the proposed methods with different levels of modelling detail that can be found in the IIW recommendations. For thin-walled structures there are methods suggested in technical papers [18]–[21] but implementation in the engineering codes has not been done.

2.3 IIW recommendations

IIW [4] is summarising and validating methods, recommendations and guidelines from scientists, researchers and industry regarding fatigue evaluation of welded

structures. In the recommendations the S-N curves, modelling techniques and fatigue assessment for both global and local methods can be found. The methods require different level of geometrical detail and the methodology of stress extraction varies. The global methods employs the nominal stress which can be divided into two components as

$$\sigma_{\text{nom}} = \sigma_{\text{n}} + \sigma_{\text{b}} \tag{2.8}$$

where σ_{n} is the membrane stress and σ_{b} is the bending stress excluding local geometrical effects. The stress can be extracted from analytical expressions or from FE solvers if the stress concentration factor is known. When local effects are included, the stress components can be expressed in a linearised form based on Bernoulli's theory of beams as

$$\sigma_{\text{n}} = \frac{1}{t} \int_{z=0}^{z=t} \sigma_{\text{tot}}(z) \, \mathrm{d}z \tag{2.9}$$

$$\sigma_{\text{b}} = \frac{6}{t^2} \int_{z=0}^{z=t} (\sigma_{\text{tot}}(z) - \sigma_{\text{n}}) \left(\frac{t}{2} - z \right) \, \mathrm{d}z \tag{2.10}$$

where the structural stress is the sum of the linearised components, σ_{tot} is the actual stress distribution through the thickness and z is the distance from the plate surface. The local stress effects can be found from the integrated structural stress as

$$\sigma_{\text{nl}}(z) = \sigma_{\text{tot}}(z) - \sigma_{\text{n}} - \left(1 - \frac{2z}{t} \right) \sigma_{\text{b}} \tag{2.11}$$

where the stress component σ_{nl} is the nonlinear stress peak that is included in the notch stress approach. As can be seen from Figure 2.4 the stress at a weld contains both global and local components.

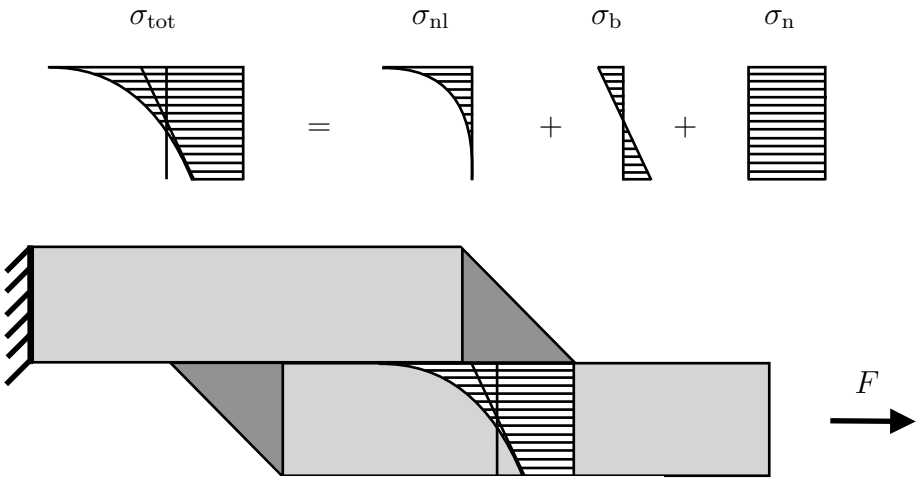

Figure 2.4: Stress distribution through thickness at a weld notch. Total stress separated into three stress components. Adapted from [4].

Depending on the way the stress is extracted, different methods with different fatigue strengths are used. Common for the methods is a fatigue strength where the local properties in the HAZ has been implicitly considered. The FAT class is given at 97.7% probability of survival and the value is geometric and loading specific for global approaches and more general for detailed methods. Common for all methods is the need for destructive testing to evaluate FAT classes. FAT classes provided in the IIW [4] and related research are derived from a large set of experiments with materials of varying grade.

2.3.1 Nominal stress method

The nominal stress method is a global method with local stress raising effects excluded from the stress state. The stress should be extracted at a characteristic length from the stress concentration by using structural mechanics based on linear elastic behaviour. For example, the stress in a beam with a normal and bending component can be determined as

$$\sigma_{\text{nom}} = \frac{F}{A} + \frac{M_{\text{b}}}{W_{\text{b}}} \tag{2.12}$$

where F is the axial force, A is the load carrying area, M_{b} is the bending moment and W_{b} is the section modulus in bending. The effect of local stress gradients are included in the FAT classes in both EC9 and IIW, hence local stress raising effects should not be considered in the stress state [1]. If cutouts or other macro-geometrical shapes are interfering with the stress state in the vicinity of the weld, the increased stress level should be included [4]. To determine the increased stress level due to macro-geometrical shapes, finite element analysis (FEA) can be used with a coarse mesh to extract the nodal force close to the weld according to the recommendations. By extracting nodal forces, stress concentration effects can be avoided [4].

A certain amount of misalignment is included in the FAT class but for a non-parallel or offset joint configuration eccentricity is to be considered with an additional stress magnification factor k_{m}. Apart from the misalignment the method has limits regarding sheet thickness and joint angle. The recommended plate thickness is $t \geq 5\,\text{mm}$ and the joint angle is specific to the joint configuration. The method is reliant on the choice of a joint specific FAT class. Joints with FAT classes defined in the IIW [4] are common joints found in the construction, marine and shipbuilding industry. The FAT classes for the studied transverse non-load-carrying tee joint and the load-carrying lap joint can be seen in Table 2.1.

Table 2.1: FAT classes for a non-load-carrying tee joint and a load-carrying lap joint in aluminium from IIW recommendations [4].

Failure mode	Parameter	Tee joint	Lap joint
Toe	FAT	36	22
Root	FAT	-	12

Based on the specific FAT class and calculated stress ranges the life can be determined from equation (2.6), with $b = 3.0$ and $b = 5.0$ for joints loaded with normal and shear stresses respectively. Because of the thickness and joint limitations the use cases in the field of automotive is limited and other fatigue assessment methods are needed. In this thesis the method will be used as a second control where applicable.

2.3.2 Notch stress approach

The notch stress approach aims to model the total stress of the notch at the weld toe and weld root. To account for the non-linear behaviour at the weld root and toe, and the irregularities of the weld, the weld contour is replaced by a fictitious notch, Figure 2.5.

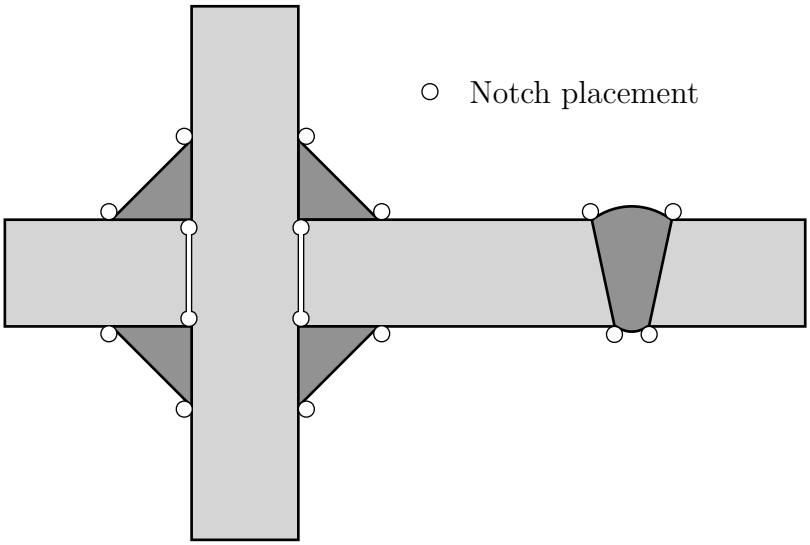

Figure 2.5: Notch placement in welded components. Adapted from [4].

Various notch radii have been suggested and tested. The IIW [4] recommends the use of fictitious notch radius $r = \rho_f = 1\,\text{mm}$ for steel and aluminium welded joints for a material thickness of $t \geq 5$ mm. The radius $r = 1\,\text{mm}$ is based on Neuber's micro-structural support theory and derived by Radaj [19]

$$r = \rho_f = \rho + s\rho^* \tag{2.13}$$

where ρ is the actual notch radii, ρ^* is the substitute micro-structural support length determined from fatigue testing of notched bars and the support factor s, depends on the strength hypothesis and loading type. "Conservative estimates, $\rho^* = 0.4$

mm, $s = 2.5$ and $\rho = 0\,\text{mm}$ (i.e. $\rho_\text{f} = 1\,\text{mm}$) have proven to be realistic for welded joints" [22].

Research shows that for thin-walled, $t < 5\,\text{mm}$, flexible structures, a notch radius of $r = 0.05\,\text{mm}$ gives sufficient results and is increasingly being used in the automotive industry [19]. In contrast to $r = 1$ mm, $r = 0.05\,\text{mm}$ is based on Creager and Paris' relation between the stress-intensity factor and the notch stress and also Irwin's theory of crack blunting [19]. The radius $r = 0.05\,\text{mm}$ is a compromise between applicable FE modelling and calculation of reasonable notch stresses at a specific stress intensity [19].

Both $r = 1$ and $r = 0.05\,\text{mm}$ are found from experiments to exist in welds. The methods do not take crack growth from surface roughness or embedded defects into account and misalignment needs to be addressed in the FE model. To bridge the gap between thin and thick-walled structures a third notch radius has been introduced $r = 0.3\,\text{mm}$ for material thickness $3 \leq t \leq 8\,\text{mm}$ [20].

The notch stress approach is an idealisation of the weld geometry. The evaluated stresses can not be directly measured in the welded component [4]. To evaluate the fatigue life with the notch stress method, specific FAT classes are used that have been calibrated against extensive testing. The FAT classes are independent of joint type but specific to different materials and radii.

In life prediction of the notch stress approach the maximum principal stress σ_1 at the notch is used with the respective FAT class. For 2D FE models plain strain condition is used and σ_1 is computed from

$$\sigma_1 = \max\left[\boldsymbol{\sigma} = \frac{\sigma_\text{x} + \sigma_\text{y}}{2} \pm \sqrt{\left(\frac{\sigma_\text{x} + \sigma_\text{y}}{2}\right)^2 + \tau_\text{xy}^2}\right] \tag{2.14}$$

It is important to note the direction of σ_1, which is required to be perpendicular to the surface normal to the notch for the notch stress approach.

It is important to distinguish the effective notch method with $r = 1\,\text{mm}$ from the notch stress approach of $r = 0.3\,\text{mm}$ and 0.05 mm. The effective notch method requires only σ_1 at the notch to be used in the fatigue life assessment together with one master FAT class, since the support factor is included in the FAT71 (aluminium). For methods using smaller radii, J. Baumgartner [21] proposes the use of variable FAT classes that depend on the opening angle ω of the notch to account for support effects, see Table 2.2 and Figure 2.6.

Table 2.2: FAT classes for $r = 0.05$ mm, with $b = 5$ for normal to weld stresses and $b = 7$ for shear stresses [23]. ω is the opening angle of the notch.

Stress mode	**Parameter**	$\mathbf{0° \leq \omega \leq 90°}$	$\mathbf{90° \leq \omega \leq 135°}$	$\mathbf{135° \leq \omega \leq 180°}$
Normal to weld	FAT	200	160	112
Shear	FAT	120	90	80

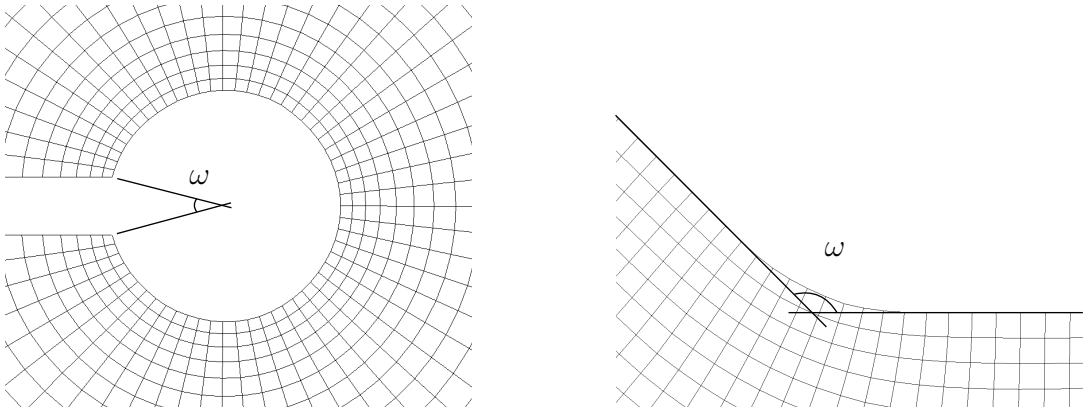

Figure 2.6: Opening angle for different notch placements.

2.4 Methods for automotive industry

Destructive testing is time consuming, costly and limits the number of design iterations. To enable a more iterative design approach with less cost, lower weight and increased durability, numerical methods in parallel with physical testing became more frequently used during the 1990s [9]. Both linear and non-linear FE models were used and the complexity of the models increased at the same rate as the computational power availability. Fatigue life prediction within automotive industry was introduced in mid-1990s based on linear static FE models and load history from measured test events [24]. At this time the majority of the fatigue failures came from welded areas but the tools for fatigue life predictions of welds were missing [9]. The first fatigue assessment method based on a unique S-N curve for welded thin-sheet structures was proposed 1995 by K. Dang Van, J-L. Fayard and A. Bignonnet [15]. The method utilises the hot-spot stress concept, hence a meshing methodology was needed to avoid stress concentrations depending on the element type and mesh size [15]. In the late 1990s a structural stress approach was introduced for fatigue life prediction of metal active gas (MAG) welds in thin steel structures [18]. The method was known as a mesh insensitive approach due to its explicit stress formulation. Instead of computing the stress state from the gradient of the nodal displacement vector with a material model for linear elasticity the structural mechanics theory was used. The method required the nodal forces and moments at the weld toe from the internal force vector $\boldsymbol{f}_{\text{int}}$. For equilibrium the linear elastic FE model can be expressed as

$$\boldsymbol{f}_{\text{int}} = \boldsymbol{K}\boldsymbol{a} = \boldsymbol{f}_{\text{ext}} \tag{2.15}$$

where $\boldsymbol{K}$ is the stiffness matrix, $\boldsymbol{a}$ is the unknown nodal displacement vector and $\boldsymbol{f}_{\text{ext}}$ is the known external force vector. Since the method does not require detailed modelling and enables sufficiently accurate results the technique has been commonly used in the automotive industry [25]. Another well-known method used for fatigue weld assessment of thin-walled structures is Dong's Approach [8] which utilises the principle of virtual work and recovers the structural stress from line forces and moments [26]. In commercial contexts the approach is referred to as the Verity

method and is used within Dassault Systèmes. Compared to the nominal and hot-spot method proposed in the IIW recommendations that uses joint specific S-N curves, Verity uses one single master S-N curve and can be used for all types of loading and joint configurations. To enable an unique master S-N curve, a stress correction based on Paris' law from fracture mechanics is used to combine the loading conditions [27]. The Volvo method utilises two S-N curves, dependent on the loading condition.

2.4.1 Volvo method

To overcome the difficulty of determining the stress state of the weld toe and weld root without considering mesh dependence, in the Volvo method nodal forces and moments are extracted. The method considers the structural stress in the elements adjacent to the weld. The structural stress is calculated as the sum of the bending stress σ_{b} and the membrane stress σ_{n} [18], shown here

$$\sigma_{\perp}(y) = \sigma_{\mathrm{b}}(y) + \sigma_{\mathrm{n}}(y) = -\frac{12 m_{\mathrm{y}}(y) z}{t^3} - \frac{f_{\mathrm{x}}(y)}{t} \tag{2.16}$$

where $\sigma_{\perp}$ is the structural stress perpendicular to the weld line, m_{y} is the line moment and f_{x} is the line force. The distance from the mid surface to the local z-coordinate is denoted as z while the element thickness is t. Since the stress is recovered from nodal forces and moments, local effects due to geometry, distortions and residual stresses from welding are not included. However, the stresses recovered explicitly have been proven to be the stress state relevant for fatigue failures [18], since the weld defects are included in the S-N curves. The line moment and force can be obtained from the nodal moment M_{y} and nodal force N_{x} of any element $\mathrm{E}^{(i)}$ at any location y [18] as

$$m_{\mathrm{y}}^{(i)}(y) = \frac{2}{l_{\mathrm{y}}^{(i)}} \left[M_{\mathrm{y1}}^{(i)} \left(1 - \frac{y}{l_{\mathrm{y}}^{(i)}} \right) + M_{\mathrm{y2}}^{(i)} \frac{y}{l_{\mathrm{y}}^{(i)}} \right] \tag{2.17}$$

$$f_{\mathrm{y}}^{(i)}(y) = \frac{2}{l_{\mathrm{y}}^{(i)}} \left[N_{\mathrm{x1}}^{(i)} \left(1 - \frac{y}{l_{\mathrm{y}}^{(i)}} \right) + N_{\mathrm{x2}}^{(i)} \frac{y}{l_{\mathrm{y}}^{(i)}} \right] \tag{2.18}$$

where the superscript defines the element identity, and the first and second subscript defines the direction and node identity, respectively. The element length along the toe is defined as $l_{\mathrm{y}}^{(i)}$ and is the absolute distance between the grid points. The moment varies linearly along the element and the extreme values at the grid points can be found as

$$m_{\mathrm{y}}^{(i)}(0) = m_{\mathrm{y1}}^{(i)} = \frac{2}{l_{\mathrm{y}}^{(i)}} M_{\mathrm{y1}}^{(i)} \tag{2.19}$$

$$m_{\mathrm{y}}^{(i)}(l_{\mathrm{y}}^{(i)}) = m_{\mathrm{y2}}^{(i)} = \frac{2}{l_{\mathrm{y}}^{(i)}} M_{\mathrm{y2}}^{(i)} \tag{2.20}$$

$$f_{\mathrm{x}}^{(i)}(0) = f_{\mathrm{x1}}^{(i)} = \frac{2}{l_{\mathrm{y}}^{(i)}} N_{\mathrm{x1}}^{(i)} \tag{2.21}$$

$$f_{\mathrm{x}}^{(i)}(l_{\mathrm{y}}^{(i)}) = f_{\mathrm{x2}}^{(i)} = \frac{2}{l_{\mathrm{y}}^{(i)}} N_{\mathrm{x2}}^{(i)} \tag{2.22}$$

To capture the maximum structural stress the bending stress is extracted at the top surface, $z = t/2$. This is done for both grid points in element $\mathrm{E}^{(i)}$ by inserting the extreme values in equation (2.16) such that

$$\sigma_{\perp}(0) = -\frac{12M_{\mathrm{y1}}^{(i)}}{l_{\mathrm{y}}^{(i)}t^2} - \frac{2N_{\mathrm{x1}}^{(i)}}{l_{\mathrm{y}}^{(i)}t} \tag{2.23}$$

$$\sigma_{\perp}(l_{\mathrm{y}}^{(i)}) = -\frac{12M_{\mathrm{y2}}^{(i)}}{l_{\mathrm{y}}^{(i)}t^2} - \frac{2N_{\mathrm{x2}}^{(i)}}{l_{\mathrm{y}}^{(i)}t} \tag{2.24}$$

For each node with two adjacent elements there will be two stress values. In the algorithm the maximum value with maintained sign is used

$$\max\left[\sigma_{\perp}(l_{\mathrm{y}}^{(i)}),\ \sigma_{\perp}(0^{(i+1)})\right] \tag{2.25}$$

Also, for corners and weld ends the maximum value with maintained sign are used. In those areas four different stress values are calculated to capture the different scenarios for the three adjacent elements $\mathrm{E}^{(1)}$, $\mathrm{E}^{(2)}$ and $\mathrm{E}^{(3)}$, see Figure 2.7.

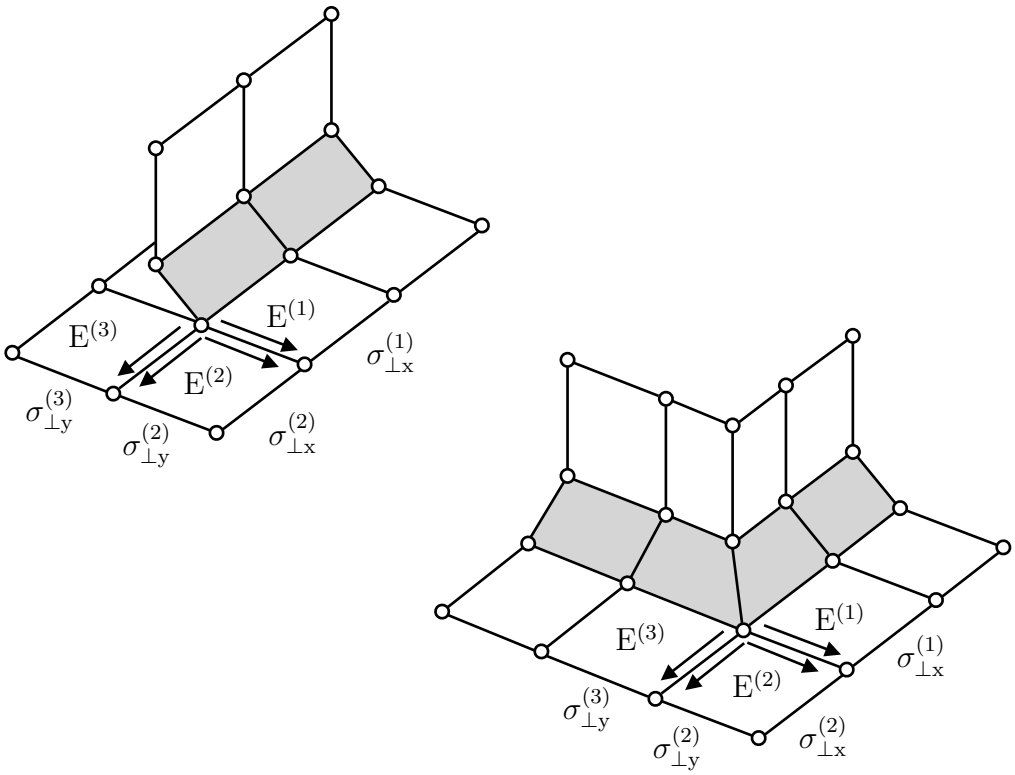

Figure 2.7: FE representation of a weld end and a sharp corner, modelled according to the Volvo method. Adapted from [18].

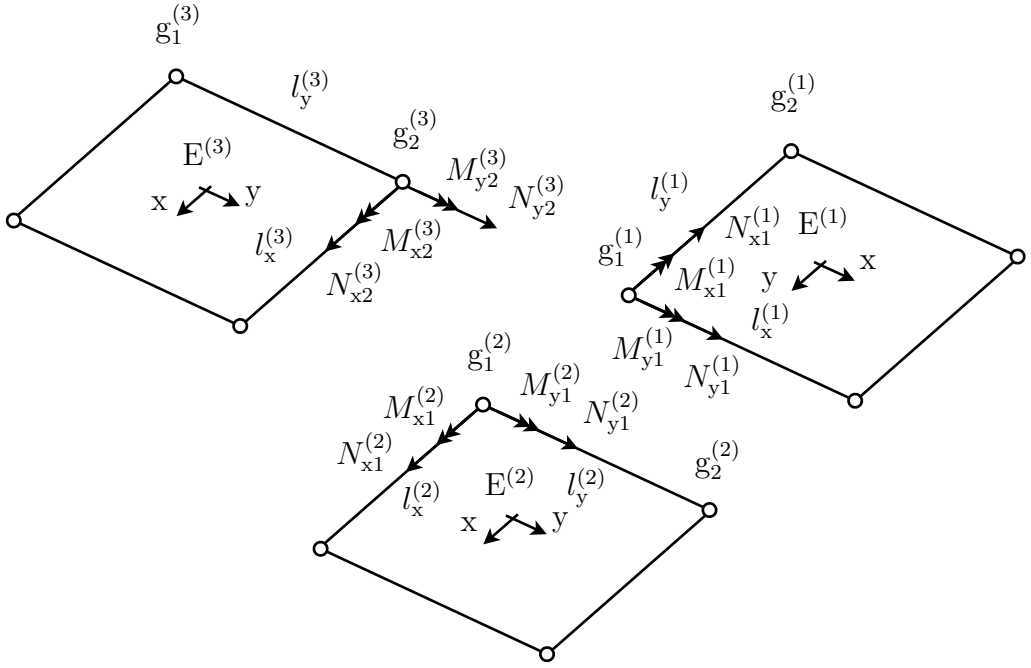

Figure 2.8: Free-body diagram of the three adjacent elements to the weld start/end or sharp corner representing forces, moments and element length used in the calculations with the Volvo method. g_1 and g_2 represent the grid point identity for each element along the weld line. Adapted from [18].

The stresses with respect to the sharp element corner $E^{(2)}$ can be found as

$$\sigma_{\perp x}^{(2)} = \frac{12M_{x1}^{(2)}}{l_x^{(2)}t^2} - \frac{2N_{y1}^{(2)}}{l_x^{(2)}t} \tag{2.26}$$

$$\sigma_{\perp y}^{(2)} = -\frac{12M_{y1}^{(2)}}{l_y^{(2)}t^2} - \frac{2N_{x1}^{(2)}}{l_y^{(2)}t} \tag{2.27}$$

The original approach does not consider any averaging of the grid point forces and moments. Later research showed that false positive failures at weld ends could be avoided by averaging the line force and moments [28]. By combing equations (2.19)−(2.22) the value can be evaluated at the middle of the weld toe as

$$m_y^{(i)} = \frac{m_y^{(i)}(0) + m_y^{(i)}(l_y^{(i)})}{2} \tag{2.28}$$

$$f_x^{(i)} = \frac{f_x^{(i)}(0) + f_x^{(i)}(l_y^{(i)})}{2} \tag{2.29}$$

The averaging was also shown to decrease the overall mesh sensitivity [28]. After the averaging the stress perpendicular to the weld toe for an element $E^{(i)}$ can be expressed as

$$\sigma_{\perp,\mathrm{top}}^{(i)} = \frac{6m_{\mathrm{y}}^{(i)}}{t^2} + \frac{f_{\mathrm{x}}^{(i)}}{t} \tag{2.30}$$

$$\sigma_{\perp,\mathrm{bot}}^{(i)} = -\frac{6m_{\mathrm{y}}^{(i)}}{t^2} + \frac{f_{\mathrm{x}}^{(i)}}{t} \tag{2.31}$$

Cycles under variable-amplitude loading conditions are proposed to be defined with RFC and the partial damage should be accumulated with Palmgren–Miner linear damage rule [26], see equation (2.7).

2.4.1.1 Bending ratio

The method utilises two master S-N curves independent of material grade and joint configuration, one for loading dominated by bending and the second dominated by membrane stresses [29]. It has been seen that joints loaded in bending have an increased fatigue resistance compared to joints stressed in tensile loading [18]. In general for an element, the ratio β between the bending stress and the structural stress is defined as

$$\beta = \frac{|\sigma_{\mathrm{b}}|}{|\sigma_{\mathrm{b}}| + |\sigma_{\mathrm{n}}|} \tag{2.32}$$

In the original approach the recommendation was to use the membrane S-N curve if $0 \leq \beta \leq 0.5$ and the bending S-N curve if $0.5 < \beta \leq 1$. Later in both OptiStruct and nCode DesignLife an interpolation between the curves is performed if the average bending ratio $\overline{\beta}$ is greater than a defined critical bending ratio β_{c}, usually $\beta_{\mathrm{c}} = 0.5$. Depending on the choice of solver the average bending ratio over the load history is calculated in different ways. For OptiStruct [13] the average bending ratio for each element is calculated as

$$\overline{\beta}_{\mathrm{OS}}^{(i)} = \frac{\sum_{j=1}^{k} \beta_j \left(\sigma_{\perp,\mathrm{top}}^2\right)_j}{\sum_{j=1}^{k} \left(\sigma_{\perp,\mathrm{top}}^2\right)_j} \tag{2.33}$$

In nCode DesignLife [30] an equivalent stress is used for the calculation of the element-wise average bending ratio

$$\overline{\beta}_{\mathrm{nC}}^{(i)} = \frac{\sum_{j=1}^{k} \beta_{\mathrm{eq},j} \left(\sigma_{\mathrm{eq,top}}^2\right)_j}{\sum_{j=1}^{k} \left(\sigma_{\mathrm{eq,top}}^2\right)_j} \tag{2.34}$$

The equivalent bending ratio is defined as

$$\beta_{\mathrm{eq}} = \frac{|\sigma_{\mathrm{eq,top}} - \sigma_{\mathrm{eq,bot}}|}{|\sigma_{\mathrm{eq,top}} + \sigma_{\mathrm{eq,bot}}| + |\sigma_{\mathrm{eq,top}} - \sigma_{\mathrm{eq,bot}}|} \tag{2.35}$$

where the equivalent stress is determined based on the maximum absolute principal stress as

$$\sigma_{\mathrm{eq,top}} = \max\left[\boldsymbol{\sigma} = \frac{\sigma_{\mathrm{xx}} + \sigma_{\mathrm{yy}}}{2} \pm \sqrt{\left(\frac{\sigma_{\mathrm{xx}} - \sigma_{\mathrm{yy}}}{2}\right)^2 + \sigma_{\mathrm{xy}}^2}\right] \tag{2.36}$$

$$\sigma_{\mathrm{eq,bot}} = \frac{\sigma_{\mathrm{xx}} + \sigma_{\mathrm{yy}}}{2} + \frac{\sigma_{\mathrm{xx}} - \sigma_{\mathrm{yy}}}{2} \cos(\phi_{\mathrm{p}}) + \sigma_{\mathrm{xy}} \sin(\phi_{\mathrm{p}}) \tag{2.37}$$

where the orientation ϕ_{p}, of the maximum principal stress is calculated from the following relation

$$\tan(2\phi_{\mathrm{p}}) = \frac{2\sigma_{\mathrm{xy}}}{\sigma_{\mathrm{xx}} - \sigma_{\mathrm{yy}}} \tag{2.38}$$

3

Modelling and Analysis

The individual parts implemented in the study are described in this chapter. This includes two weld geometries, the fatigue loading and the material parameters, and also the steps taken to implement the three methods studied and the cases studied to compare the methods.

3.1 Geometry

Two joints were studied, the tee joint and the lap joint. These joints were chosen because of their different characteristics. The tee joint is a non-load carrying stiffener with mainly tensile and compressive load while the lap joint is a load carrying joint also affected by bending due to the asymmetry of the joint. In Figure 3.1 the geometries are presented, and the parameters used are shown in Table 3.1.

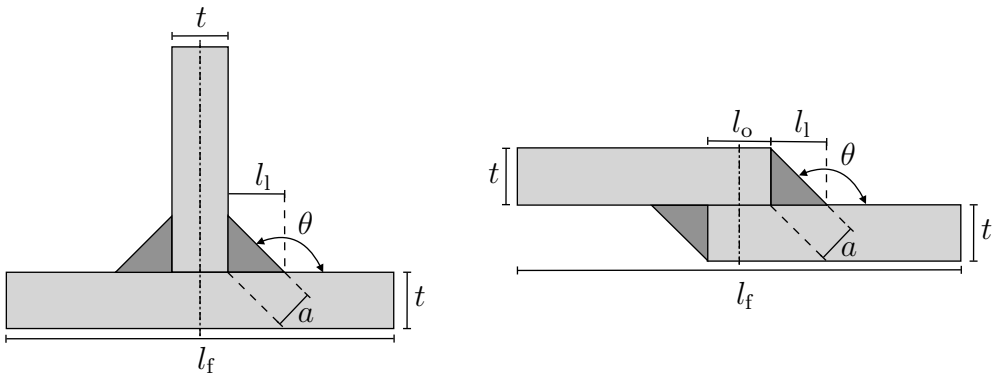

Figure 3.1: Geometrical representation of tee joint on the left hand side and the lap joint to the right.

Table 3.1: Parameters used in the reference weld. Weld length and plate width are the same for all geometries.

Description	Parameter	Value	Unit
Free length	l_f	180	mm
Leg length	l_l	3	mm
Overlap length	l_o	20	mm
Plate thickness	t	3	mm
Plate width	w	50	mm
Theoretical throat	a	2.12	mm
Weld angle	θ	135	deg
Weld length	l_w	50	mm

3.2 Loading and material

The variable amplitude loading used for the fatigue assessment was generated using a random number generator in Python. The peak values were established using normal distribution with a mean value of 0.0 and a standard deviation of 0.2. In OptiStruct RFC is integrated in the solver, while a RFC algorithm for the nominal stress method was created. From the RFC, 99 cycles were identified and the range and mean value can be seen in Figure 3.2.

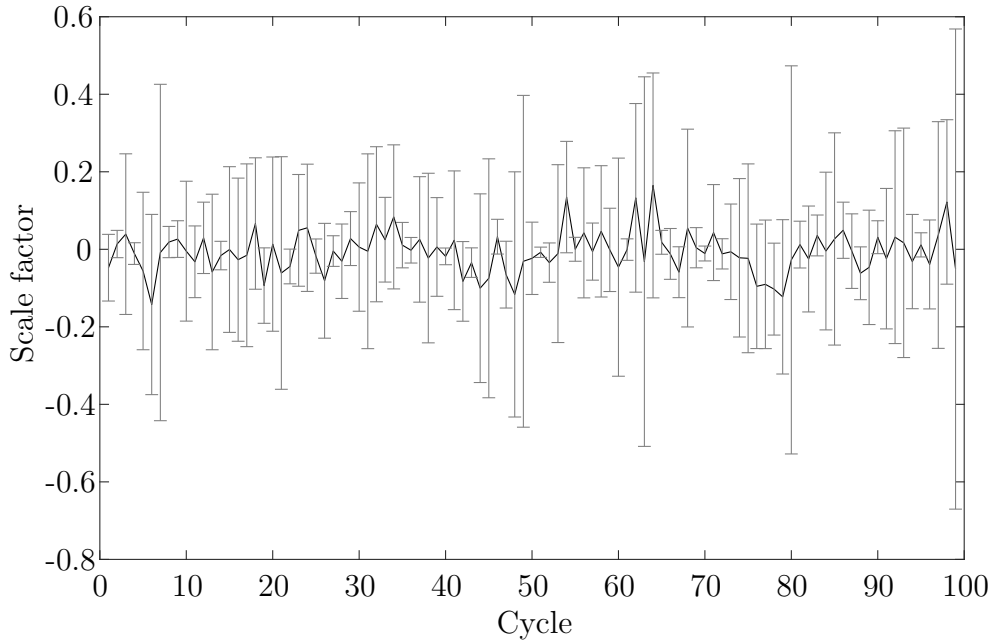

Figure 3.2: Range and mean values used for load scaling.

For the three methods the range was used to scale the stress state from the applied static reference load, 10.0 kN and 2.5 kN for the tee joint and lap joint respectively. To ensure HCF loading conditions, the largest stress range was limited by $N_\mathrm{f}(\Delta\sigma_\mathrm{max}) > 10^4$.

The mechanical properties for the aluminium used in the fatigue assessment study can be seen in Table 3.2. The material has been modelled with an isotropic and homogeneous linear elastic material model. The S-N curves used for the different methods are presented in the respective section.

Table 3.2: Material properties used for weld joint modelling.

Description	Parameter	Value	Unit
Young's modulus	E	70.0	GPa
Poisson's ratio	ν	0.3	-

3.3 Nominal stress method

The nominal stress method is both joint and loading specific and can be used without any additional FE software. To make the method more time efficient the calculations were performed in Python. The stress range was calculated for each cycle, the life was found from equation (2.6) and the damage was summed for the load sequence following equation (2.7). The methodology used is illustrated in Figure 3.3. For each joint and failure mode the process was repeated.

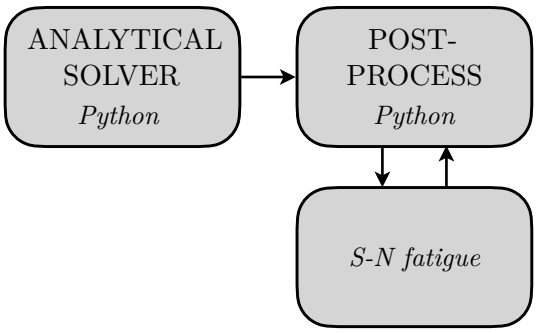

Figure 3.3: Work flow using Python for the nominal stress method.

3.3.1 Modelling

The method does not require any pre-processing but the geometry was considered to correctly calculate the nominal stress. For toe failures the stress was calculated from equation (2.12) by considering the axial force and the cross-sectional area of the plate. For the root failures the same equation was used but the stress was calculated based on the total load carrying weld area. The area was defined as the effective throat, times the weld length. Note that the effective throat is twice the theoretical throat for the lap joint, see Figure 3.1. To account for the secondary bending stress

due to the plate offset of the lap joint the stress magnification factor, $k_{\mathrm{m}} = 2.5$, was used based on equation (3.1) expressed in IIW [4]

$$k_{\mathrm{m}} = 1 + \lambda \frac{eL_1}{t(L_1 + L_2)} \tag{3.1}$$

where e is the plate offset, L_1 and L_2 is respective plate length and λ is a restraint dependent factor. The joint was assumed to be fully restrained, hence $\lambda = 3$.

3.3.2 S-N curve

The nominal stress method considers geometrical stress raising effects in the FAT class and examines toe and root failure separately. Since the tee joint is non-load carrying, root failure is not included. For the lap joint both toe and root failure are included. Hence three different S-N curves were used to perform the fatigue assessment with the nominal stress method, see Figure 3.4.

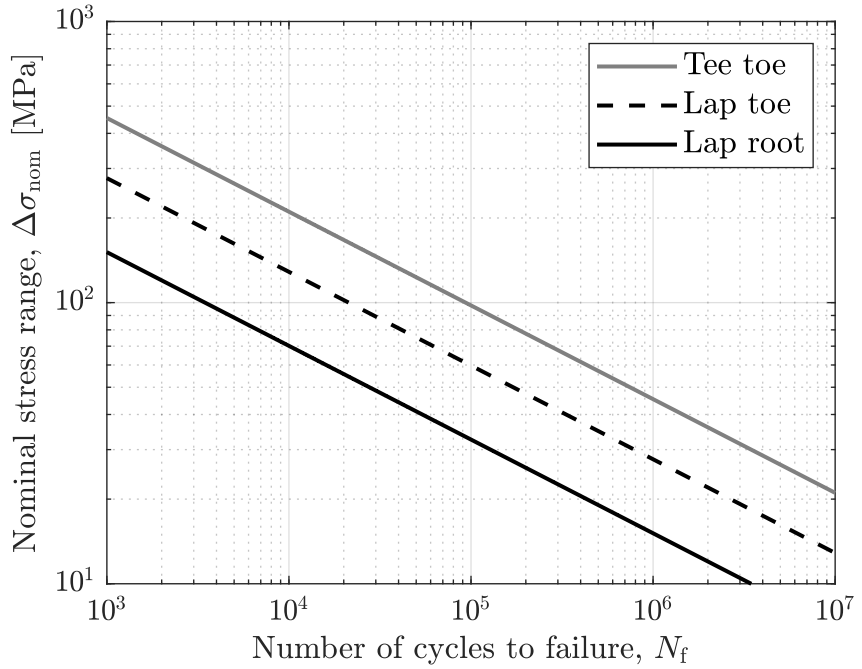

Figure 3.4: S-N curves for the two studies joints. Nominal stress range versus Number of cycles to failure for aluminium structure with $t \geq 5$ mm.

3.4 FEA methods

Both the notch stress approach and Volvo method utilise FEM to model the weld and surrounding area. The boundary conditions are the same while the modelling detail, S-N curve and stress extraction differs.

3.4.1 FE boundary conditions

The joints were loaded with a variable amplitude loading and converted into load cycles, see Figure 3.2. The static reference load was applied at node A and C depending on study and joint, see Figure 3.5 - 3.6. Rigid body elements (RBE2) were used to connect the structure to the Dirichlet and Neumann boundary conditions at node A, B and C defined in section 3.5.

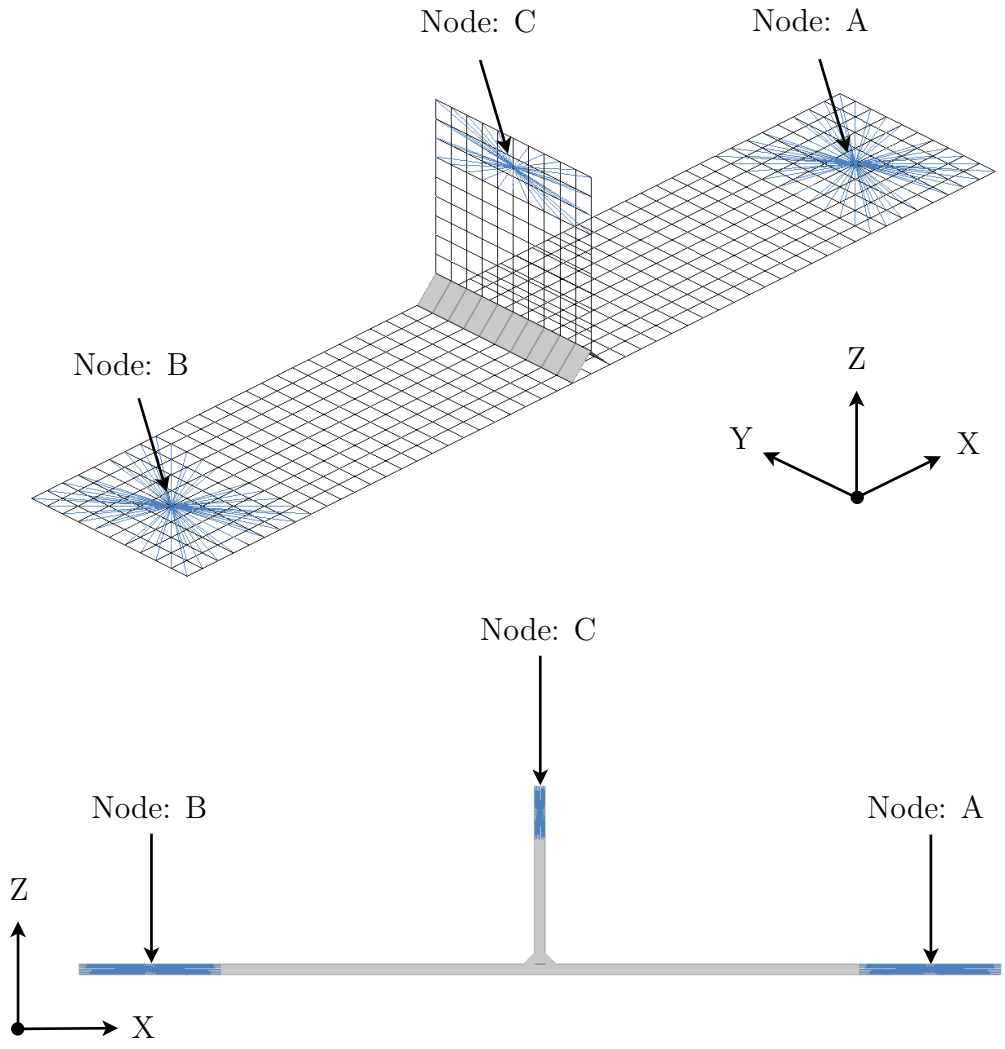

Figure 3.5: FE representation of tee joint used for the Volvo method and notch stress method. The blue elements represent RBE2 couplings.

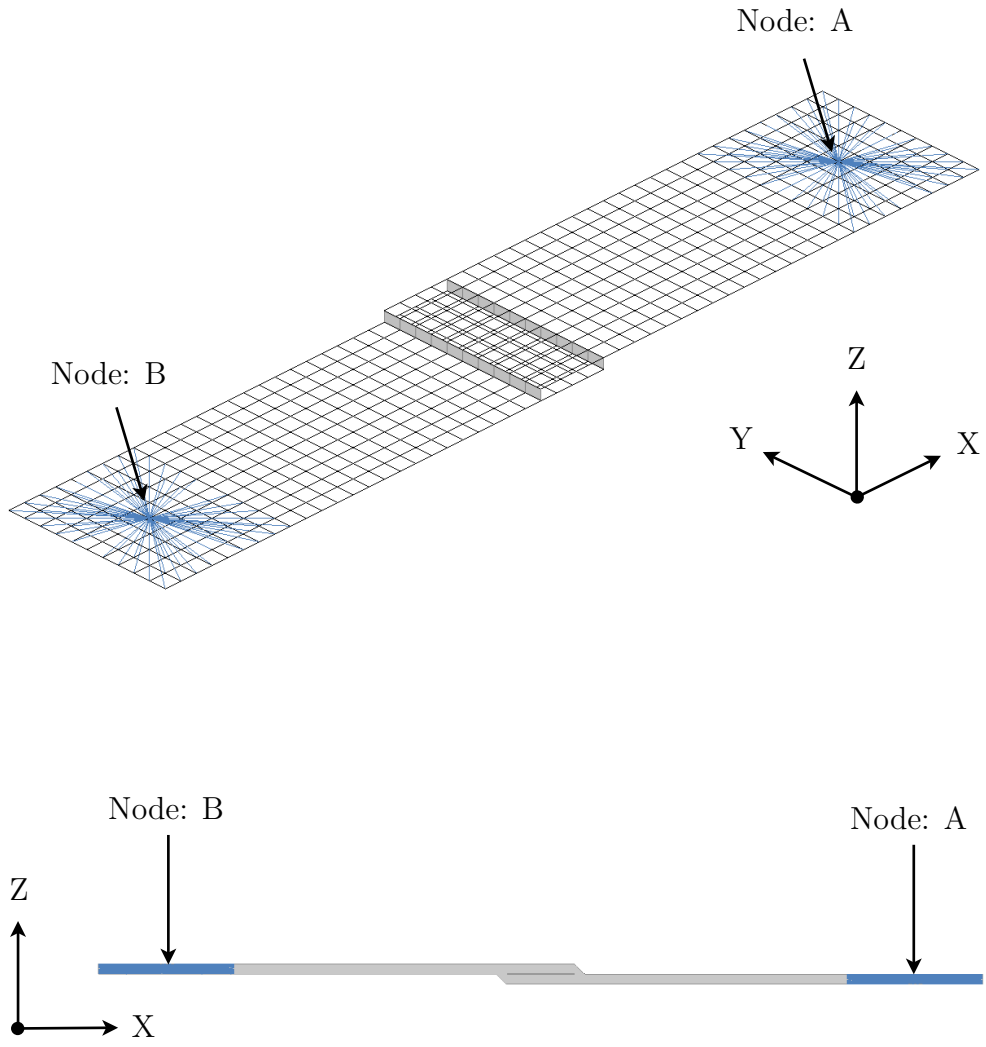

Figure 3.6: FE representation of lap joint used for the Volvo method and notch stress method. The blue elements represent RBE2 couplings.

3.4.2 Notch stress approach

In the following section the modelling procedures for the notch stress approach are discussed. Depending on factors such as the joint complexity and model size, different modelling approaches might be used, see Figure 3.7.

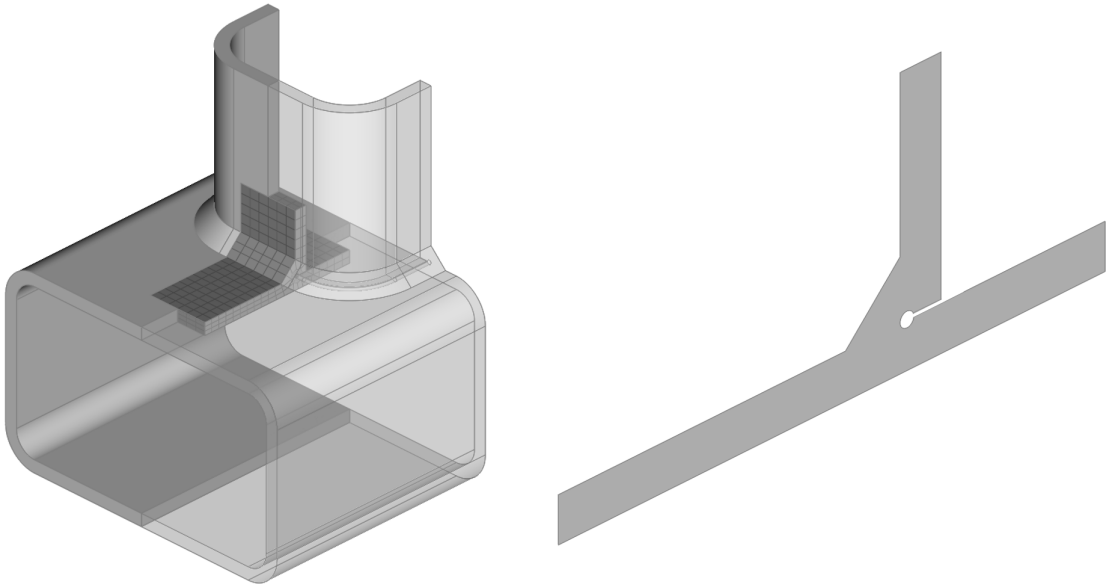

Figure 3.7: Examples of possible mesh configurations. Complete solid structure, solid sub section or 2D shell section.

Because of the constant cross sectional weld geometry in the studied joints, the notch stress approach was implemented in 2D using shell elements with plain strain condition. The geometry was pre-processed in ANSA, OptiStruct was used as fatigue solver and post-processing was performed in META, see Figure 3.8.

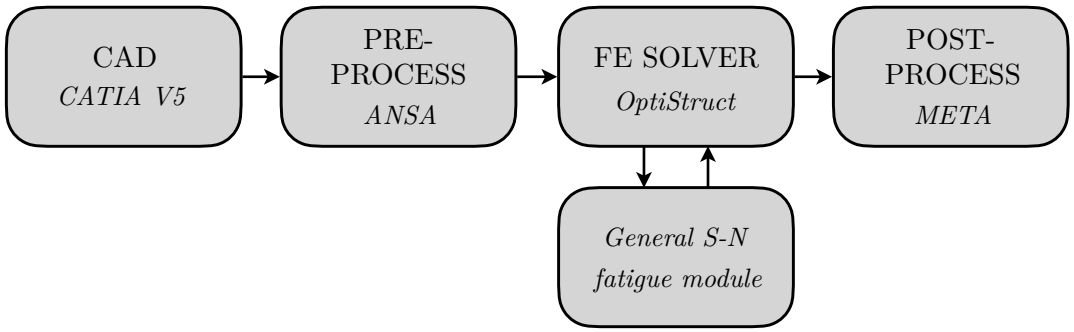

Figure 3.8: Work flow using notch stress approach.

3.4.2.1 Mesh

To implement the notch stress approach in FEA a sufficiently fine mesh needs to be used so that the stress at the notch converges. Modelling recommendations by the IIW [4] are presented in Table 3.3, the accuracy depending on element choices and

quality is discussed at length in [31]. It is of importance to implement the modelling recommendations not only for the notch but to also extend them a characteristic length along the edge of the weld and base material.

Table 3.3: Modelling recommendations for implementation of the notch stress approach in FEA [4].

Element type	Relative size	Elements in 45° arc	Elements in 360° arc
Quadratic elements	$\leq r/4$	≥ 3	≥ 24
Linear elements	$\leq r/6$	≥ 5	≥ 40

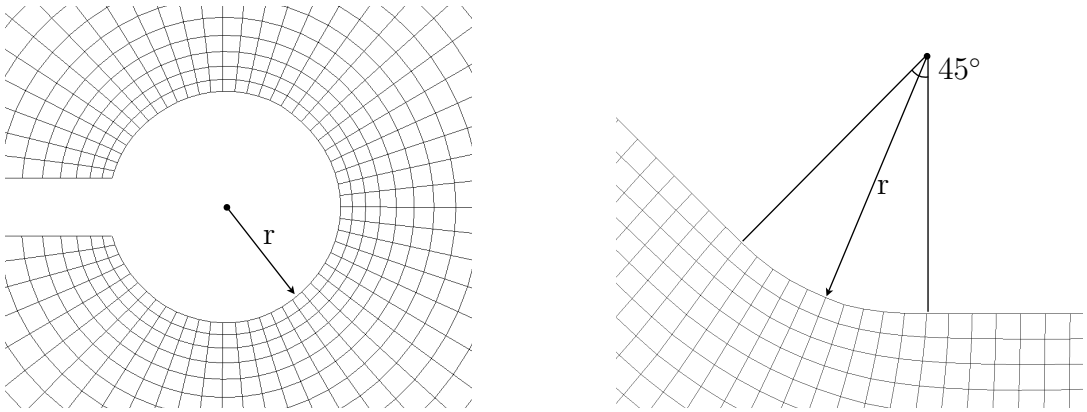

Figure 3.9: Notch mesh example, showing the converged mesh for nodal maximum first principal stress at the notches for $r = 0.05$ mm.

The notch stress method relies on the nodal first principal stress, OptiStruct was limited to the use of element stress in the fatigue module. Thus the mesh size used in the study needed to be refined significantly to reduce the stress gradient in the elements at the notch. To find an adequate local mesh size a convergence study was performed of the element and nodal first principal stress at the notch, starting with the mesh as recommended by IIW, see Table 3.3. The nodal stress level at a mesh size of 0.25 µm was used as reference, the convergence requirement set was an error $< 2\%$. Furthermore, each analysis used in the study was checked such that the relative error between the nodal and element stress was below the convergence requirement. This was done since the stress gradient in the element depends on how the load is applied.

Each joint was modelled in ANSA using first order quadrilateral shell elements (CQUAD4) with 6 degrees of freedom per node formulation and supplemented by linear triangular shell elements (CTRIA3) where necessary. Plain strain condition was assumed and a global element size of 0.5 mm was used. To capture the peak stress, an element size according to the convergence study presented in section 4.1 was used in the vicinity of the notch. The resulting models are shown below, see Figure 3.10−3.11.

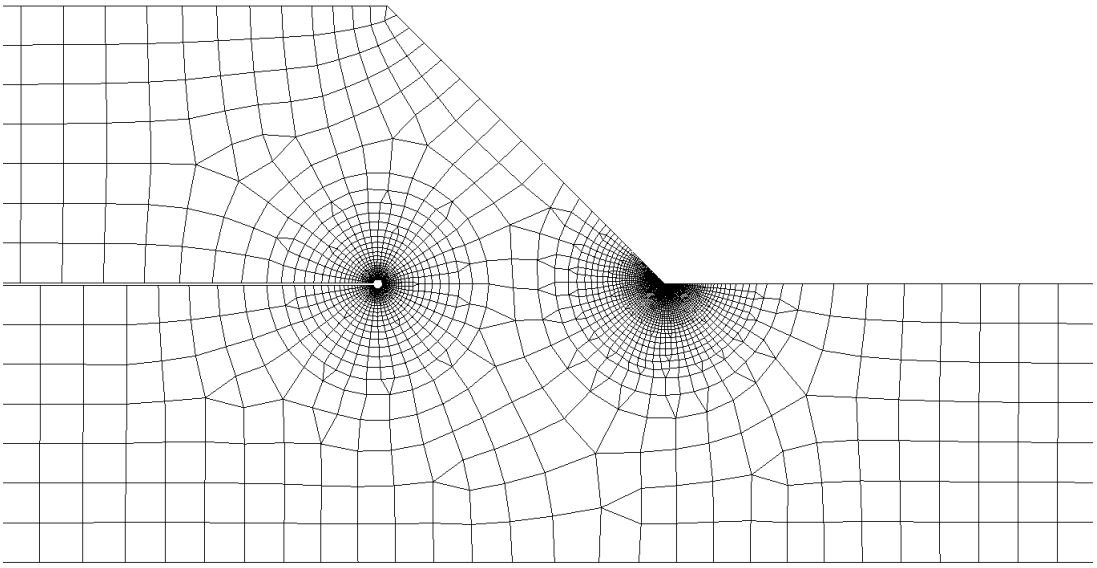

Figure 3.10: Lap joint FE representation with element size according to convergence study at the notch and global element length $l < 0.5$ mm.

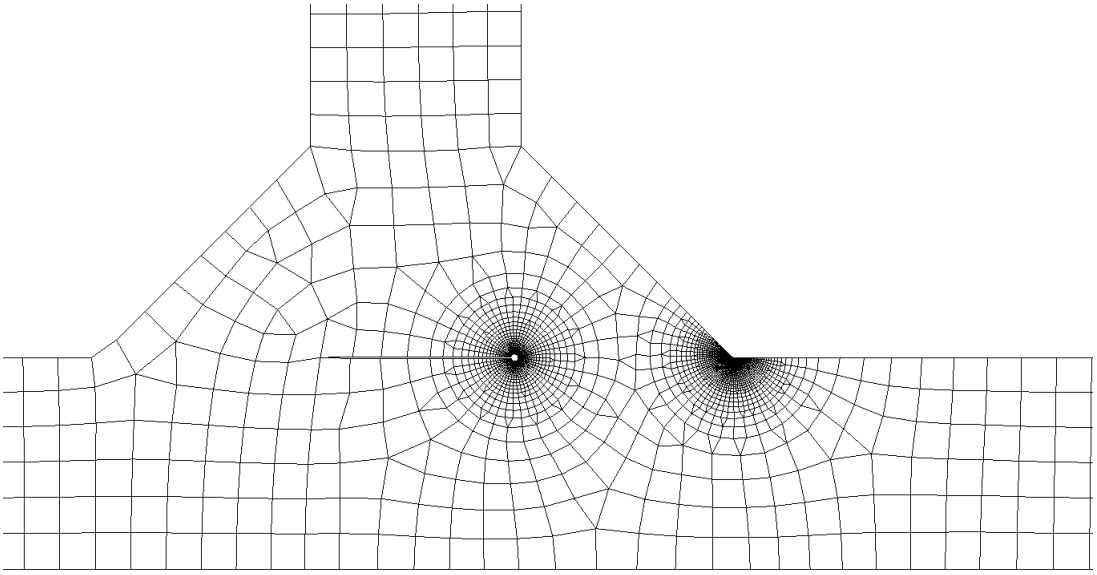

Figure 3.11: Tee joint FE representation with element size according to convergence study at the notch and global element length $l < 0.5$ mm.

3.4.2.2 S-N curve conversion

For the notch stress approach the fatigue resistance data is defined as the FAT class at $N_\mathrm{f} = 2 \cdot 10^6$. To enable fatigue life simulations in OptiStruct the fatigue strength coefficient was converted from the FAT class to the definition of the corresponding parameter in OptiStruct as

$$\left.\begin{aligned} \Delta\sigma &= \sigma'_{\mathrm{f}}\ N_{\mathrm{f}}^{-1/b} \\ \Delta\sigma &= FAT\left(\tfrac{N_{\mathrm{f}}}{2\cdot 10^6}\right)^{-1/b} \end{aligned}\right\} \sigma'_{\mathrm{f}} = \frac{FAT}{(2\cdot 10^6)^{-1/b}} \tag{3.2}$$

Depending on opening angle and stress mode different fatigue resistance is used, see Table 3.4. For the tee joint and lap joint two different material cards were used. The different material zones can be seen in Figure 3.12.

Table 3.4: Fatigue strength coefficient used in OptiStruct for $r = 0.05$ mm, where ω is the opening angle of the notch and σ'_{f} have units of MPa.

Stress mode	**Parameter**	$\mathbf{0° \leq \omega \leq 90°}$	$\mathbf{90° \leq \omega \leq 135°}$
Normal to weld	σ'_{f}	3641	2913

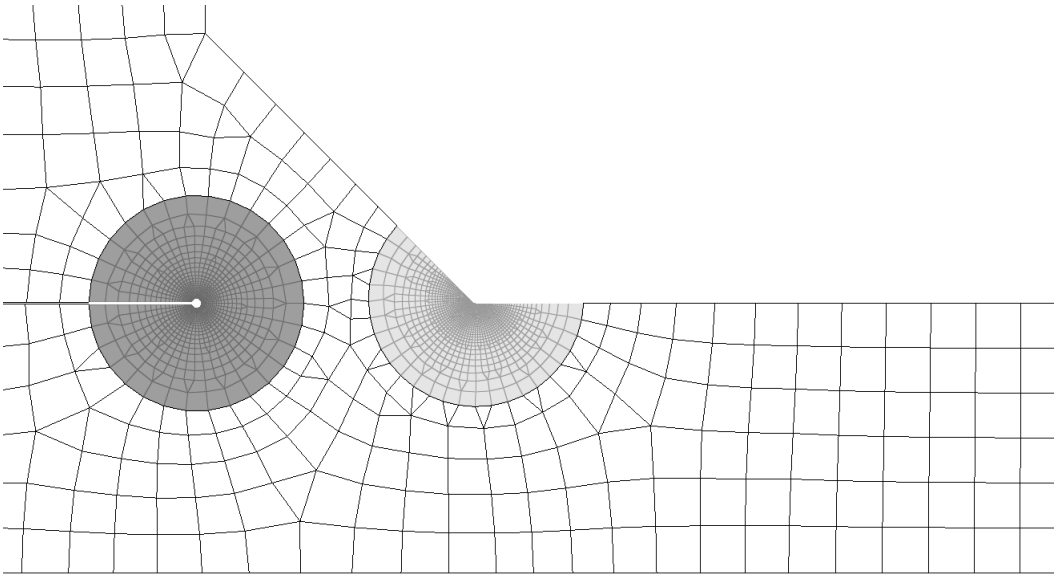

Figure 3.12: Material zones for tee joint in OptiStruct with dark grey representing root, light grey representing toe and white representing parent material.

3.4.3 Volvo method

In the following section the modelling procedures for the Volvo method are discussed. The method is capable of handling multiple welded joints modelled in three-dimensional space using shell elements. The mean surface of the geometry was studied with a relatively coarse mesh. The weld elements were defined separately and referred to a parameter and property identification card. The elements were defined with a material card including two S-N curves to be used in the seam weld fatigue solvers. OptiStruct was mainly used to study the joints but nCode DesignLife was used to extract the average bending ratio which is not possible in OptiStruct. When nCode DesignLife was used, MSC Nastran [32] was used to extract nodal forces and moments. The result was posted in a compatible post-processor for the respective fatigue solver. The methodology used can be seen in Figure 3.13.

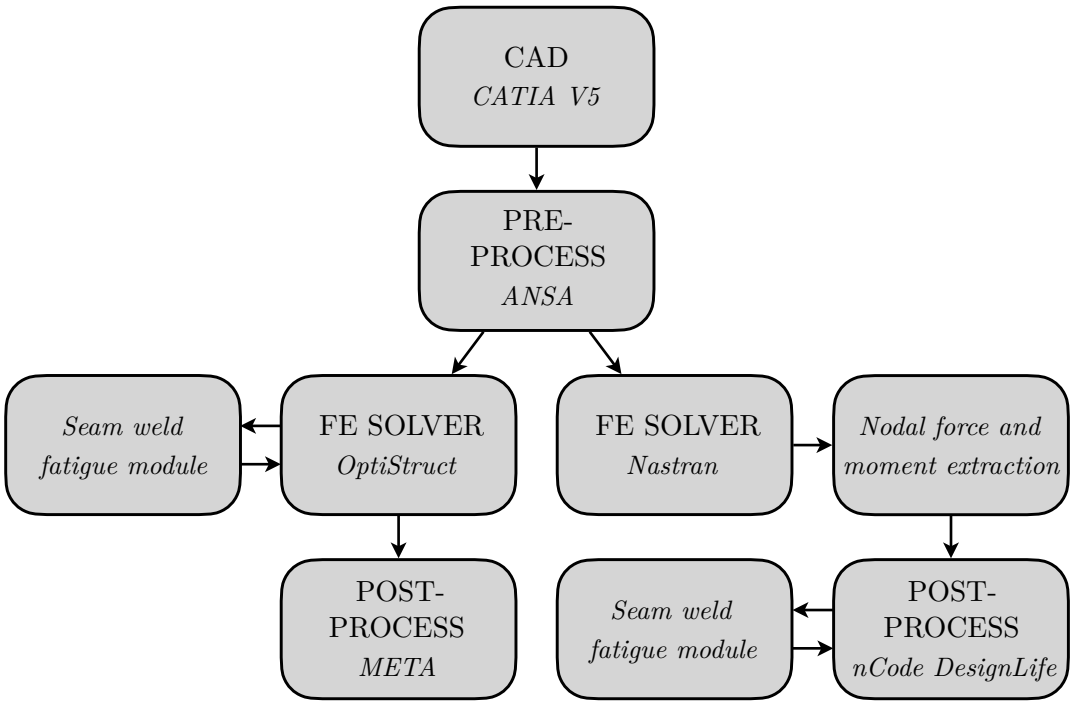

Figure 3.13: Work flow using OptiStruct and nCode DesignLife for the Volvo method.

3.4.3.1 Mesh

The method is known as a mesh independent approach with sufficient accuracy. However, six mesh rules were proposed to get consistent results [29].

- The weld element and the structure adjacent to the weld should be modelled with quadrilateral shell elements.
- The mean surface should be used to model the structure.
- The distance between the nodes of the weld elements and the actual weld toe should be $t/2$.
- Thickness of the weld element should be modelled as the theoretical throat.
- The element length should be approximately 10 mm.
- Small radii should not be modelled.

Note that the recommended element size was initially 10 mm but has been adjusted to $4-5$ mm to adequately capture the curvature of a complex geometry [33]. The studied geometries were meshed with an element size of 5 mm and the element type used for the analysis was CQUAD4, see Figure 3.14−3.15.

To capture the stiffness of the weld, the lap joint was meshed with a one row element

overlap at each weld location while the tee joint was modelled with two rows of weld elements with an angle of 45°. The weld elements were modelled with the theoretical throat and the element normal was pointing towards the weld toe.

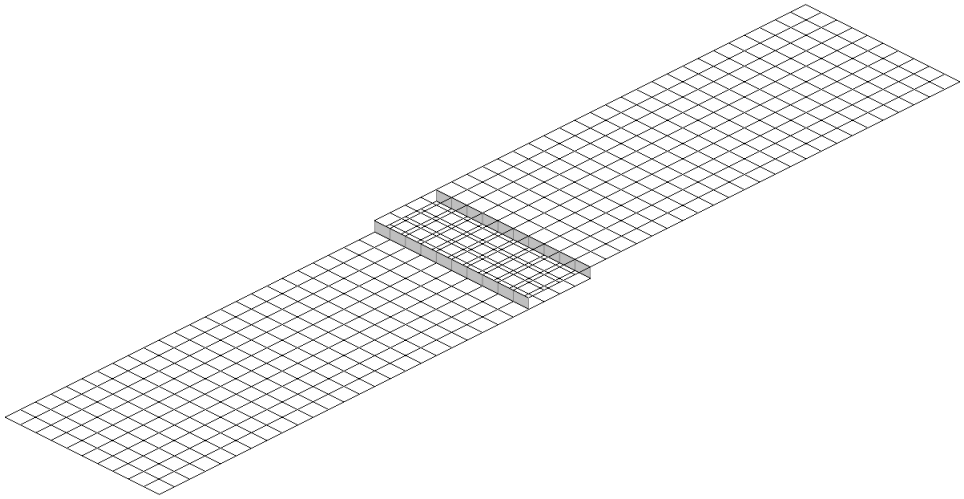

Figure 3.14: Lap joint FE representation with element size 5 mm, with grey elements representing the weld elements.

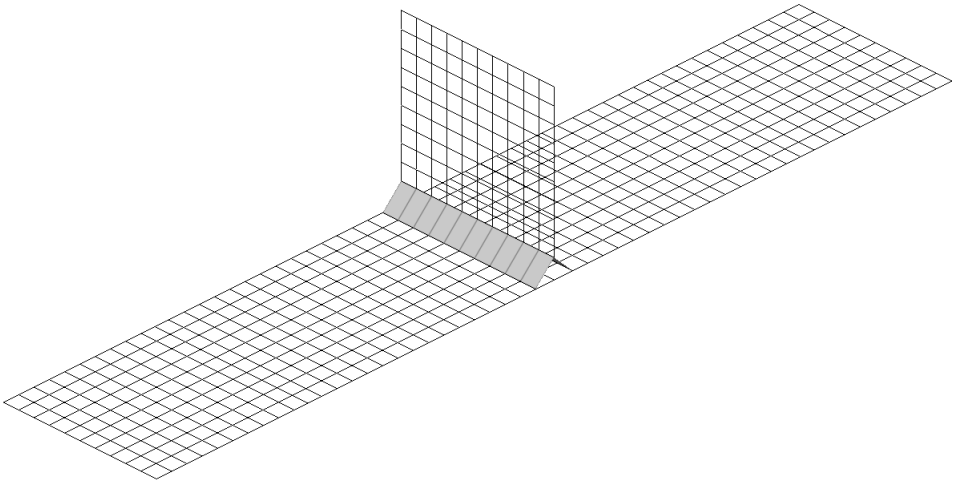

Figure 3.15: Tee joint FE representation with element size 5 mm, with grey elements representing the weld elements.

3.4.3.2 S-N curve extraction

Due to lack of fatigue material data for thin-walled aluminium structures the material properties were exacted from a log-log S-N plot generated by M. Fermér and H. Svensson [33], see Figure 3.16. The data represents two general S-N curves based on

thin-sheet aluminium alloys at a load ratio $R = -1$ from eight different specimens with a thickness of 2.0 and 3.0 mm.

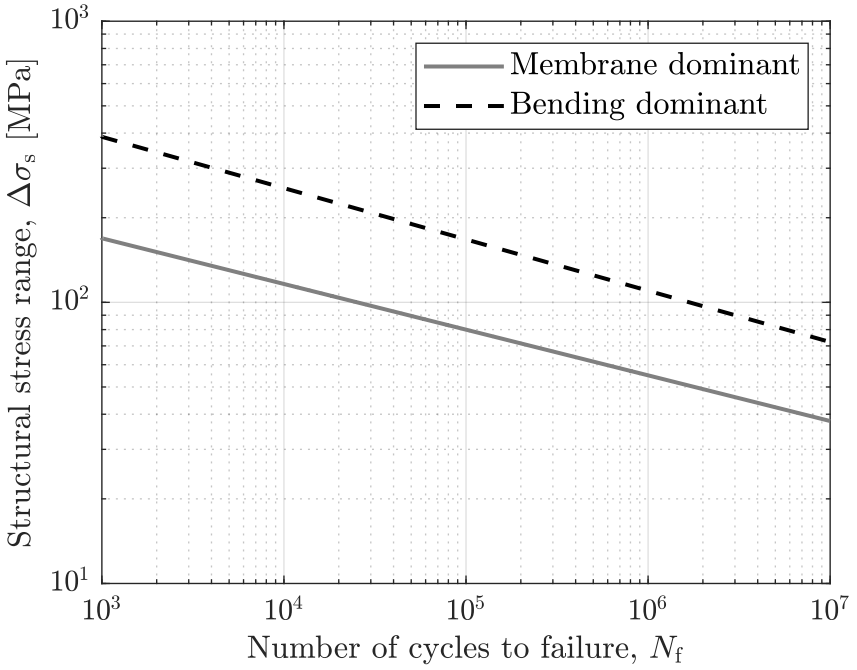

Figure 3.16: S-N curves for Volvo method. Structural stress range versus number of cycles to failure for thin-walled aluminium structure. Adapted from [33].

Since the fatigue strength coefficient and the first fatigue strength exponent were missing in the plot, the parameters were extracted with the use of a power law function

$$y = ax^k \tag{3.3}$$

The variables can be replaced by the relevant fatigue parameters and transformed from the log-log domain to the equation of a straight line in order find the slope b of the curve

$$\Delta\sigma = \sigma'_f \ N_f^{-1/b} \tag{3.4}$$

$$\log(\Delta\sigma) = \log(\sigma'_f) - b^{-1} \ \log(N_f) \tag{3.5}$$

$$b^{-1} = -\frac{Y_2 - Y_1}{X_2 - X_1} \tag{3.6}$$

where X and Y is defined as

$$X = \log(N_f), \quad Y = \log(\Delta\sigma) \tag{3.7}$$

Hence, b can be calculated as

$$b^{-1} = -\frac{\log(\Delta\sigma_2) - \log(\Delta\sigma_1)}{\log(N_{f,2}) - \log(N_{f,1})} = -\frac{\log(\Delta\sigma_2/\Delta\sigma_1)}{\log(N_{f,2}/N_{f,1})} \tag{3.8}$$

Finally the fatigue strength coefficient can be found as

$$\sigma'_{\mathrm{f}} = \frac{\Delta\sigma}{N_{\mathrm{f}}^{-1/b}} \tag{3.9}$$

The fatigue strength coefficient and fatigue strength exponent were modified to match a 97.7% probability of survival, same as for the given FAT classes used in the nominal and notch stress methods. The extracted modified material data can be seen in Table 3.5. The critical bending ratio used for interpolation between the curves was defined as $\beta_{\mathrm{c}} = 0.5$.

Table 3.5: Fatigue resistance constants for thin-walled aluminium structure used in the Volvo method defined at $N_{\mathrm{f}} = 1$. Where σ'_{f} have units of MPa and b is dimensionless.

Loading condition	$\boldsymbol{\sigma'_{\mathrm{f}}}$	$\boldsymbol{b}$
Membrane	519	6.2
Bending	1369	5.5

3.5 Analysis

To perform the comparison study of the Volvo method and notch stress method, four different cases were defined. Case 1 and 2 were defined as stated in the IIW recommendations with axial loading and were compared with the nominal stress method. Case 3 and 4 were defined with varying loading conditions to capture the bending sensitivity.

3.5.1 Case 1

Case 1, fatigue assessment of the tee joint, was defined as the structural detail 511 in the IIW recommendations. Both ends of the longitudinal plate were attached to RBE2 elements with the master nodes A and B, see Figure 3.5. Single-point constraints (SPC) at node A and B were defined to constrain the motion, see Table 3.6. The static load applied at node A can be seen in Table 3.7.

Table 3.6: Dirichlet boundary conditions used in FEA for tee joint in case 1.

Node	**Translation SPC**	**Rotation SPC**
A	Y, Z	MX, MY, MZ
B	X, Y, Z	MX, MY, MZ
C	-	-

Table 3.7: Neumann boundary condition used in FEA for tee joint in case 1.

Node	**Magnitude**	**Unit**	**Direction**
A	10.0	kN	X

3.5.2 Case 2

Case 2, fatigue assessment of the lap joint, was defined as the structural detail 614 in the IIW recommendations. Both plate ends were attached to RBE2 elements with the master nodes A and B, see Figure 3.6. SPC at nodes A and B were defined equivalent as for case 1, see Table 3.8. Due to the plate offset of the lap joint the static load was reduced compared to case 1 to stay within the boundary of HCF. The load applied at node A can be seen in Table 3.9.

Table 3.8: Dirichlet boundary conditions used in FEA for lap joint in case 2.

Node	Translation SPC	Rotation SPC
A	Y, Z	MX, MY, MZ
B	X, Y, Z	MX, MY, MZ

Table 3.9: Neumann boundary condition used in FEA for lap joint in case 2.

Node	Magnitude	Unit	Direction
A	2.5	kN	X

3.5.3 Case 3

To study the effect of the distance between the supports of the lap joint, case 3 was defined. Same load and boundary conditions as for case 2 was used. The difference was the free length l_f between the RBE2 couplings, see Figure 3.6. The varying free length can be seen in Table 3.10. In general for lap joints the bending ratio is around 0.7 [34]. For the Volvo method, β_c was set to 0.5. To investigate the influence of the interpolation between the S-N curves, a separate simulation with one master S-N curve was analysed. The fatigue resistance constants from the membrane loading condition were used, see Table 3.5.

Table 3.10: Varying distance between the supports used in FEA for lap joint in case 3.

Load case	l_f	Unit
1	180.0	mm
2	160.0	mm
3	140.0	mm
4	120.0	mm
5	100.0	mm
6	80.0	mm
7	60.0	mm

3.5.4 Case 4

Case 4 was defined to study the effect of a combined stress state in the tee joint, from a bending ratio $\beta = 0$ to $\beta = 1$. The model configuration used for the bending sensitivity study can be seen in Figure 3.5. Same boundary conditions as for load case 1 was used, see Table 3.6. In order to vary the bending ratio an additional force vector was defined in node C. The force applied at nodes A and C respectively can be seen in Table 3.11. To exclude the interference of the different characteristics of the S-N curves used for the two numerical methods an additional analysis was performed. The analysis was performed using a calibrated master S-N curve of the Volvo method. The S-N curve was calibrated against the notch stress method such that both methods produced the same number of sequences to failure N_s at $F_\mathrm{X} = 10\,\mathrm{kN}$ with the same slope. Resulting in the slope $b = 5$ and the fatigue strength coefficient $\sigma_\mathrm{f}' = 819$.

Table 3.11: Varying Neumann boundary condition used in FEA for tee joint in case 4.

	Node A			Node C		
Load case	**Magnitude**	**Unit**	**Direction**	**Magnitude**	**Unit**	**Direction**
1	10.0	kN	X	0.0	N	Z
2	9.0	kN	X	20.0	N	Z
3	8.0	kN	X	40.0	N	Z
4	7.0	kN	X	60.0	N	Z
5	6.0	kN	X	80.0	N	Z
6	5.0	kN	X	100.0	N	Z
7	4.0	kN	X	120.0	N	Z
8	3.0	kN	X	140.0	N	Z
9	2.0	kN	X	160.0	N	Z
10	1.0	kN	X	180.0	N	Z
11	0.0	kN	X	200.0	N	Z

4

Results

In the following sections the results from the convergence study and fatigue analysis are presented. The analysis is performed according to the methods presented in section 3.5. The results of the fatigue analysis are focused on the relative difference between the methods. The difference is presented as the deviation from the results of the notch stress method. Excluding the nominal stress method the simulations using FEA showed the weld toe as the initial fatigue failure location, hence toe failure is exclusively discussed.

4.1 Convergence study

The results from the convergence study showed that a mesh size at the notch of 0.5 µm fulfils the requirement, the study is presented in Table 4.1 and Figure 4.1.

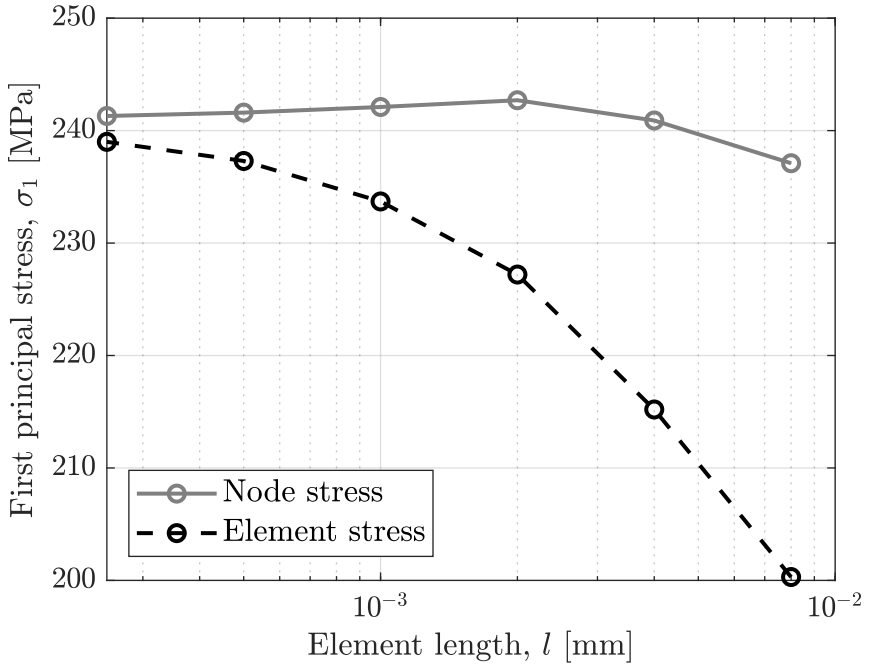

Figure 4.1: Convergence study of the notch stress method. Nodal stress and element stress.

Table 4.1: Convergence study of notch stress approach with linear shell elements. Stress extracted from nodes and elements.

	8 µm	**4 µm**	**2 µm**	**1 µm**	**0.5 µm**	**0.25 µm**	**Unit**
Nodal stress	237.1	240.9	242.7	242.1	241.6	241.3	MPa
Convergence error	1.74	0.17	−0.58	−0.33	−0.12	-	%
Element stress	200.3	215.2	227.2	233.7	237.3	239	MPa
Convergence error	16.99	10.82	5.84	3.15	1.66	0.95	%

4.2 Case 1

In case 1 the fatigue life of the non-load carrying tee joint was analysed using the nominal stress method, the notch stress approach and the Volvo method. The life was measured as the number of sequences to failure and the results from the fatigue life analysis are presented in Table 4.2. The fatigue failure from the analysis appeared at the toe and the deviation between the notch stress approach and the Volvo method was 8%. The deviation of the nominal stress method was −21%. This was expected since the nominal stress method accounts for some misalignment in the S-N curve which gives conservative results for ideal welds.

Table 4.2: Results from fatigue analysis of case 1 presented in section 3.5.1. Tee joint loaded with $F_{\mathrm{X}} = 10\,\mathrm{kN}$.

Method	$\boldsymbol{N_{\mathrm{s}}}$	**Deviation**
Notch	$42 \cdot 10^3$	-
Volvo	$45 \cdot 10^3$	8%
Nominal	$33 \cdot 10^3$	−21%

4.3 Case 2

In case 2 the fatigue life prediction of the lap joint was carried out with the methods studied in case 1. The results from the fatigue life analysis are presented in Table 4.3. The results showed a larger deviation between the methods, in particular the Volvo method that deviated by 846%, see the discussion in chapter 5. The nominal stress method showed a conservative result also for case 2 with a deviation of −46%.

Table 4.3: Results from fatigue analysis of case 2 presented in section 3.5.2. Lap joint loaded with $F_{\mathrm{X}} = 2.5\,\mathrm{kN}$.

Method	$\boldsymbol{N_{\mathrm{s}}}$	**Deviation**
Notch	$57 \cdot 10^3$	-
Volvo	$542 \cdot 10^3$	846%
Nominal	$31 \cdot 10^3$	−46%

4.4 Case 3

The results from case 2 showed a larger deviation between the Volvo method and notch stress method. In case 3 the fatigue life of the lap joint was further analysed using the two methods. The obtained life from case 3 with varying l_f showed an increased fatigue resistance with a decreased l_f, see Figure 3.1 and 4.2. This is due to the stress reduction caused by the increased area moment of inertia. The difference between the methods was reduced with decreased l_f. The varying support distance also resulted in a decreased $\overline{\beta}$, see Table 4.4, since the reduced free length between the supports decreased the bending behaviour of the joint.

Table 4.4: Results from fatigue analysis of case 3 presented in section 3.5.3. Lap joint loaded with $F_X = 2.5\,\text{kN}$ with varying support distance.

Load case	$\overline{\beta}$	$N_{s,notch}$	$N_{s,Volvo}$	**Deviation**
1	0.73	$57 \cdot 10^3$	$542 \cdot 10^3$	846%
2	0.72	$64 \cdot 10^3$	$588 \cdot 10^3$	818%
3	0.71	$72 \cdot 10^3$	$648 \cdot 10^3$	773%
4	0.70	$91 \cdot 10^3$	$730 \cdot 10^3$	706%
5	0.69	$120 \cdot 10^3$	$848 \cdot 10^3$	607%
6	0.66	$183 \cdot 10^3$	$1029 \cdot 10^3$	461%
7	0.62	$365 \cdot 10^3$	$1396 \cdot 10^3$	283%

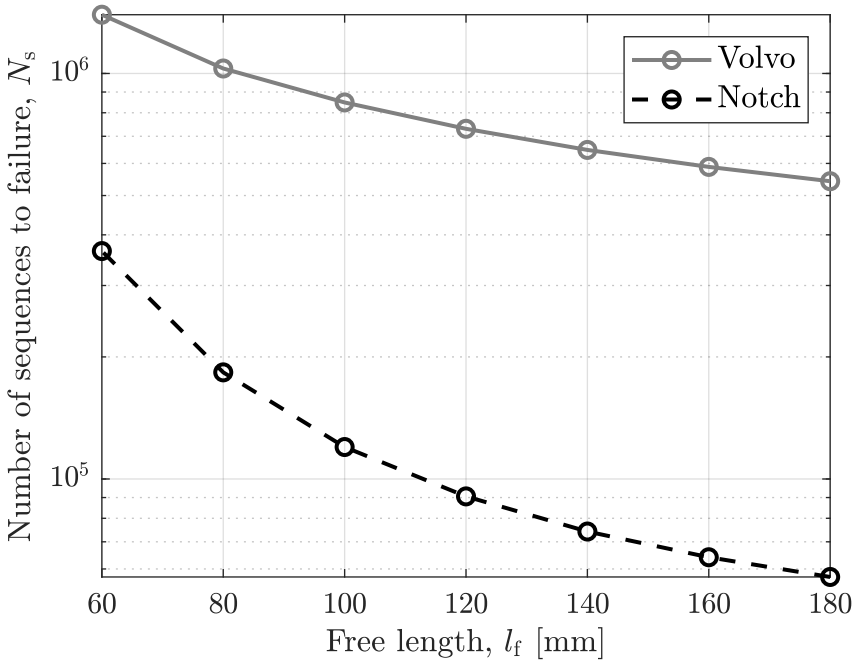

Figure 4.2: Fatigue life dependent on the free length between the supports of the lap joint.

To separate the increased life caused by the stress reduction and the variation of $\overline{\beta}$ with decreased l_f, the fatigue analysis for the Volvo method was performed with one master S-N curve based on membrane loading, $\overline{\beta} \leq \beta_\mathrm{c}$. The results showed a reduced deviation between the methods, see Table 4.5 and Figure 4.3. The deviation was within 46% to 55% and the offset is related to the fatigue strength coefficient of the methods.

Table 4.5: Results from fatigue analysis of case 3 presented in section 3.5.3. Lap joint loaded with $F_\mathrm{X} = 2.5\,\mathrm{kN}$ with varying support distance and modified S-N curve.

Load case	$\overline{\beta}$	$N_{\mathrm{s,notch}}$	$N_{\mathrm{s,Volvo}}$	**Deviation**
1	0.73	$57 \cdot 10^3$	$84 \cdot 10^3$	46%
2	0.72	$64 \cdot 10^3$	$96 \cdot 10^3$	49%
3	0.71	$72 \cdot 10^3$	$113 \cdot 10^3$	52%
4	0.70	$91 \cdot 10^3$	$140 \cdot 10^3$	54%
5	0.69	$120 \cdot 10^3$	$186 \cdot 10^3$	55%
6	0.66	$183 \cdot 10^3$	$281 \cdot 10^3$	54%
7	0.62	$365 \cdot 10^3$	$545 \cdot 10^3$	49%

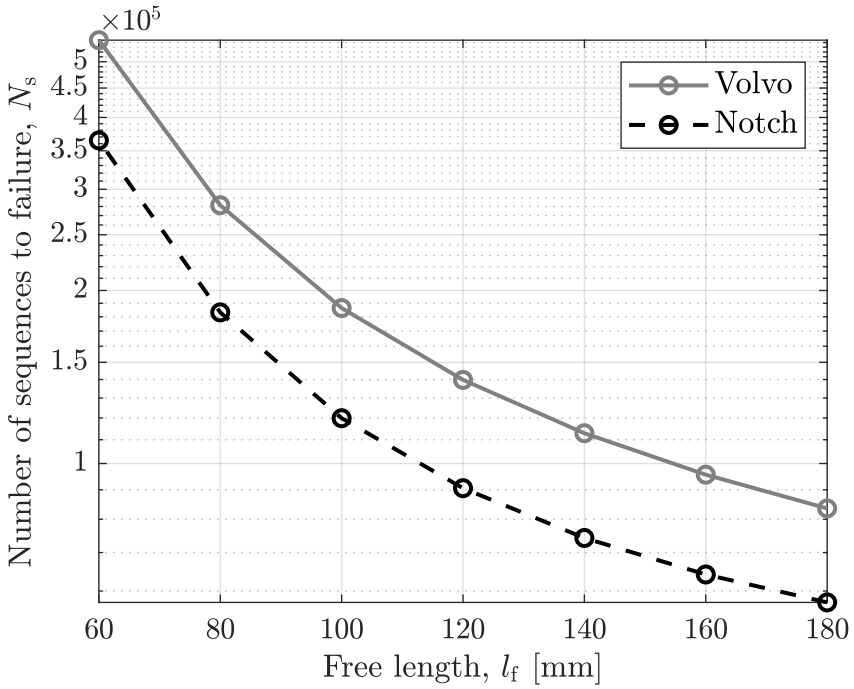

Figure 4.3: Fatigue life dependent on free length between the supports of the lap joint with modified S-N curve.

4.5 Case 4

To isolate the bending behaviour, the tee joint was loaded according to case 4 presented in section 3.5.4. The varying loading conditions resulted in a bending ratio between $\overline{\beta} = 0.01$ and $\overline{\beta} = 1.00$, see Figure 4.4.

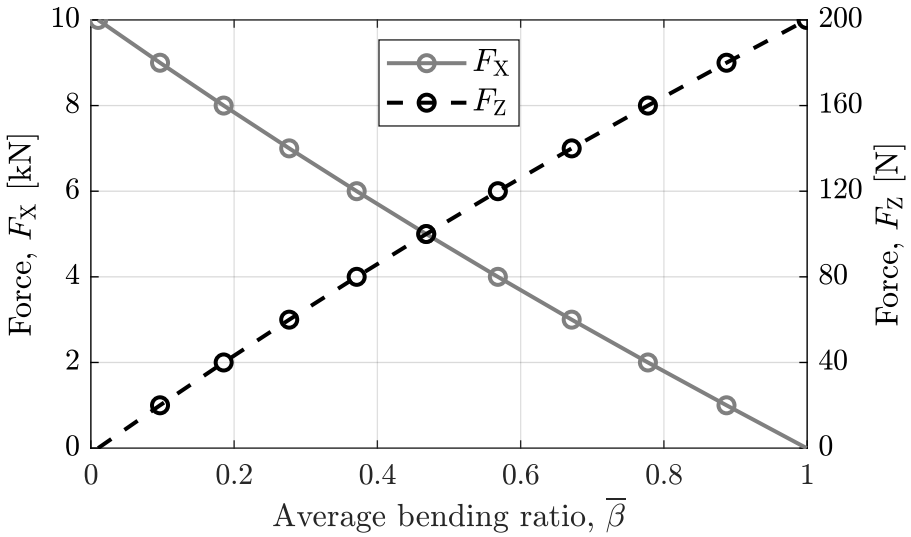

Figure 4.4: The relation between the applied loads F_X and F_Z, and the bending ratio $\overline{\beta}$.

The results presented in Table 4.6 shows an increased deviation with an increased bending ratio. In particular when the bending ratio $\overline{\beta} > \beta_c$, also shown in Figure 4.5. The behaviour occurs due to the interpolation between the two S-N curves used in the Volvo method for $\overline{\beta} > \beta_c$. Focusing on the results where $\overline{\beta} \leq \beta_c$, the deviation also varies without being affected by the interpolation.

Table 4.6: Results from fatigue analysis of case 4 presented in section 3.5.4. Tee joint loaded in varying bending ratios.

Load case	$\overline{\beta}$	$N_{s,notch}$	$N_{s,Volvo}$	**Deviation**
1	0.01	$42 \cdot 10^3$	$45 \cdot 10^3$	8%
2	0.10	$43 \cdot 10^3$	$49 \cdot 10^3$	15%
3	0.19	$44 \cdot 10^3$	$53 \cdot 10^3$	22%
4	0.28	$45 \cdot 10^3$	$58 \cdot 10^3$	30%
5	0.37	$46 \cdot 10^3$	$63 \cdot 10^3$	39%
6	0.47	$47 \cdot 10^3$	$69 \cdot 10^3$	48%
7	0.57	$48 \cdot 10^3$	$140 \cdot 10^3$	192%
8	0.67	$49 \cdot 10^3$	$356 \cdot 10^3$	626%
9	0.78	$50 \cdot 10^3$	$889 \cdot 10^3$	1671%
10	0.89	$51 \cdot 10^3$	$2176 \cdot 10^3$	4134%
11	1.00	$53 \cdot 10^3$	$5180 \cdot 10^3$	9739%

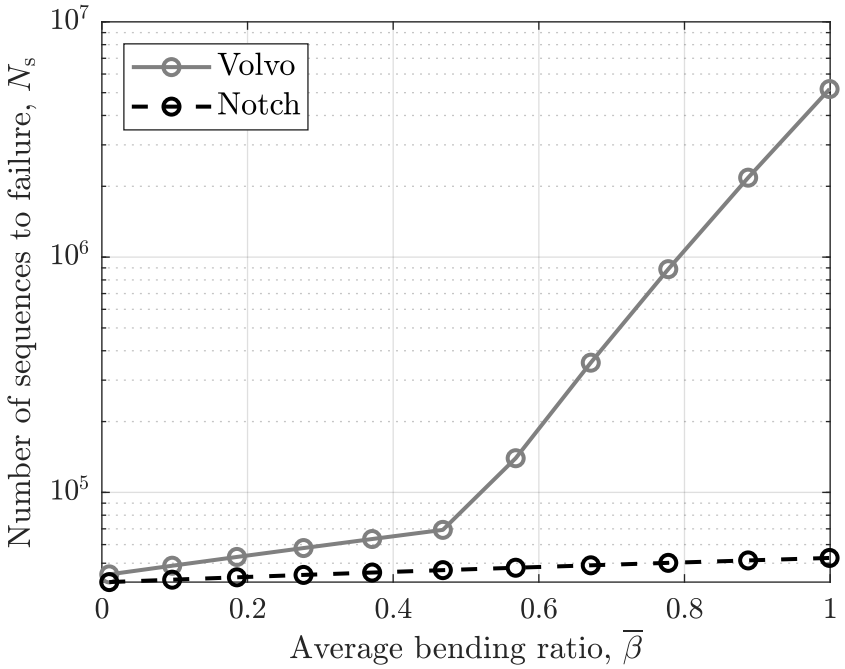

Figure 4.5: Fatigue life versus average bending ratio for tee joint.

To further investigate the behaviour without the interference of the S-N curves, one master S-N curve of the Volvo method was used. The fatigue life prediction for varying $\overline{\beta}$ shown in Table 4.7 and Figure 4.6 resulted in an increased deviation between the methods for an increased bending ratio. In Figure 4.7 the normalised stress range versus $\overline{\beta}$ is shown for the two methods. With increased bending ratio the normalised stress range was reduced at different rates. The notch stress method obtained a value of 0.954 while the normalised stress for the Volvo method was reduced to 0.863 for $\overline{\beta} = 1.00$.

Table 4.7: Results from fatigue analysis of case 4 presented in section 3.5.4. Tee joint loaded in varying bending ratios, with calibrated S-N curve for the Volvo method.

Load case	$\overline{\boldsymbol{\beta}}$	$\boldsymbol{N}_{\mathbf{s,notch}}$	$\boldsymbol{N}_{\mathbf{s,Volvo}}$	**Deviation**
1	0.01	$42 \cdot 10^3$	$42 \cdot 10^3$	0%
2	0.10	$43 \cdot 10^3$	$45 \cdot 10^3$	5%
3	0.19	$44 \cdot 10^3$	$48 \cdot 10^3$	10%
4	0.28	$45 \cdot 10^3$	$51 \cdot 10^3$	15%
5	0.37	$46 \cdot 10^3$	$55 \cdot 10^3$	21%
6	0.47	$47 \cdot 10^3$	$59 \cdot 10^3$	27%
7	0.57	$48 \cdot 10^3$	$64 \cdot 10^3$	33%
8	0.67	$49 \cdot 10^3$	$69 \cdot 10^3$	40%
9	0.78	$50 \cdot 10^3$	$74 \cdot 10^3$	48%
10	0.89	$51 \cdot 10^3$	$80 \cdot 10^3$	56%
11	1.00	$53 \cdot 10^3$	$87 \cdot 10^3$	65%

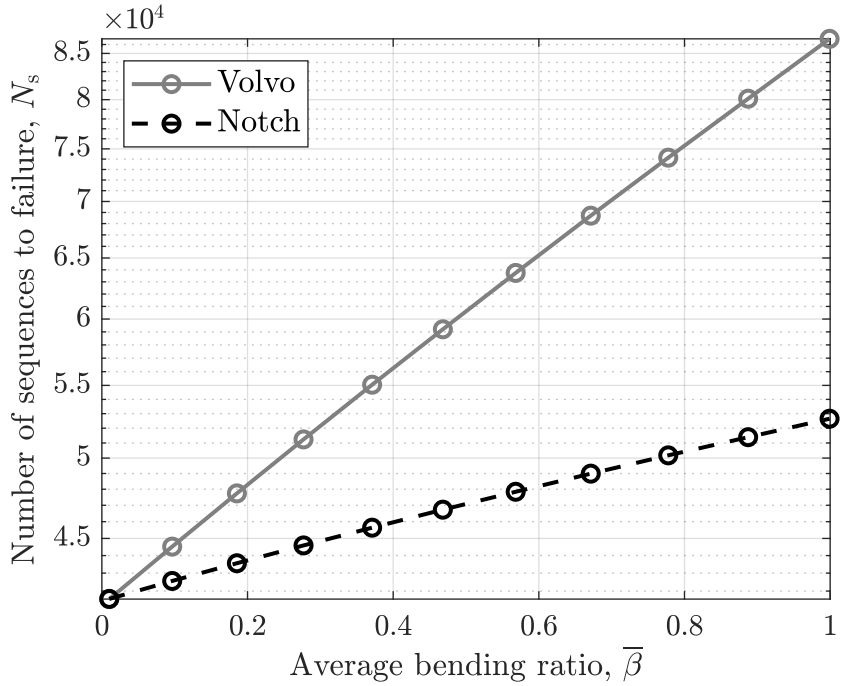

Figure 4.6: Fatigue life versus average bending ratio, with calibrated S-N curve for the Volvo method.

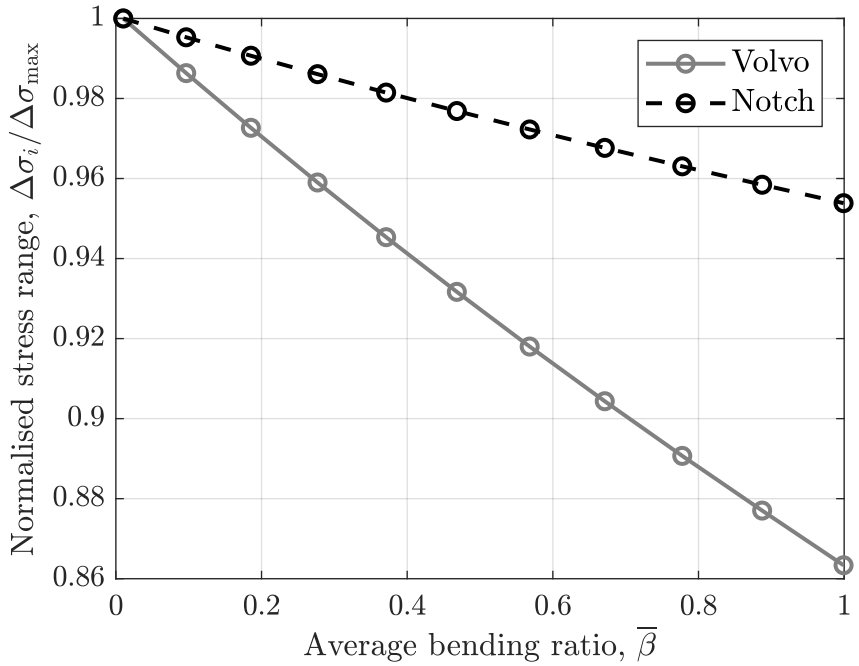

Figure 4.7: Normalised stress range versus bending ratio with values normalised with the maximum stress range for respective method.

Studying the relative stress range deviation between the methods depending on $\overline{\beta}$, a larger deviation of the stress range with an increased bending ratio was seen. This behaviour is shown in Figure 4.8, where for $\overline{\beta} = 1.00$ the relative stress range deviation was 2.7% which resulted in a life deviation of 65%, see Table 4.7. For

a constant bending ratio and a varying load magnitude the deviation between the methods is constant since a linear elastic FE model was used, see Figure 4.9.

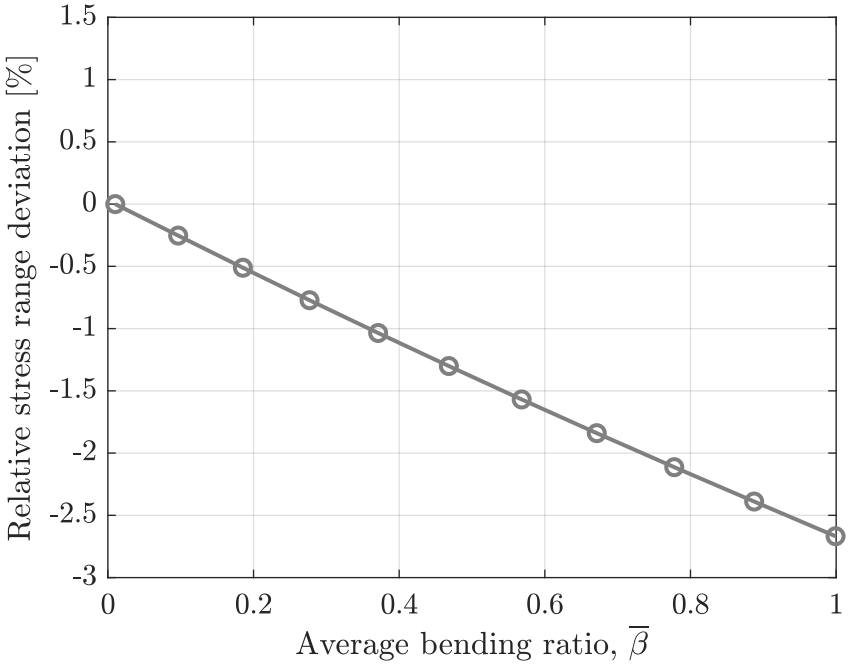

Figure 4.8: Stress range deviation between the Volvo and notch stress method with varying bending ratio.

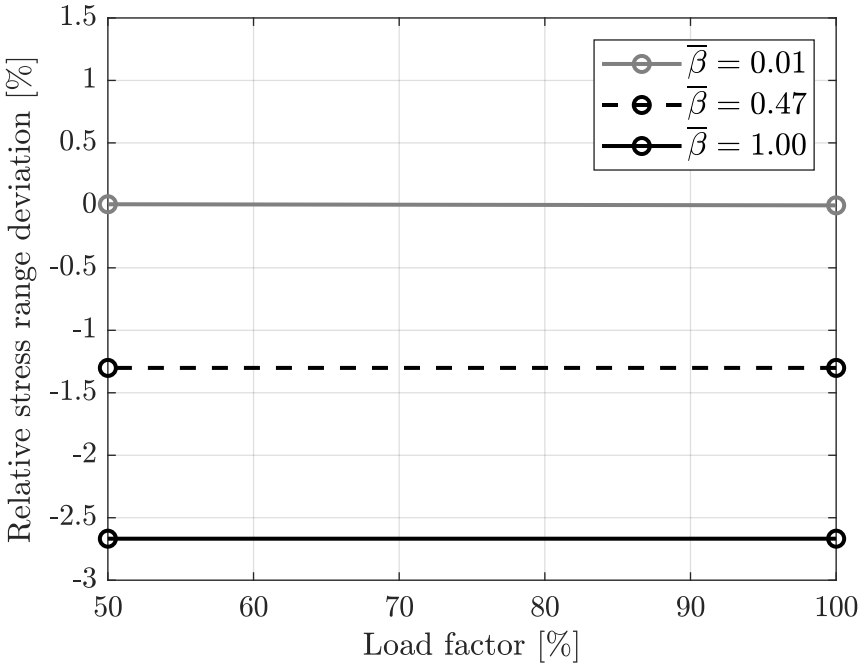

Figure 4.9: Stress range deviation between the Volvo and notch stress method with constant bending ratio and varying load magnitude.

5
Discussion

Results from the three introduced methods for the two studied welded joints have been established. The initial analysis of the tee joint in case 1 showed a small deviation between all three methods while case 2 studying the lap joint gave an increased deviation for the Volvo method. For both cases the nominal method gave conservative results. It should be mentioned that the value used as stress magnification factor, $k_{\mathrm{m}} = 2.5$, for the lap joint can be questioned. However, notable was the difference in failure location. For the nominal stress method it was observed that initial failure of the lap joint was predicted in the weld root. Both FEA methods predicted the fatigue failure in the toe. The nominal stress method developed for $t \geq 5$ mm was used as an additional reference in the comparison. In this case physical testing has indicated toe failure as the initial failure location [21].

In case 3 where the free length between the supports on the lap joint were studied, the results indicated a reduced deviation for a reduced l_{f}. The deviation is related to the bending ratio in the joint, a reduction of the bending ratio lowers the deviation between the methods. This effect is in large due to the different S-N curve designs of the Volvo and notch stress method. As stated before, the notch stress method utilises one master S-N curve. The purpose is to be joint independent but since a master S-N curve is used the fatigue prediction for bending dominated joints might be conservative. Since the S-N curve is defined such that the probability of survival for all tested joints is 97.7%, the life of some joint configurations might be excessively conservative. The Volvo method differentiates between membrane and bending dominated joints by interpolation between the membrane and bending S-N curve for $\overline{\beta} > \beta_{\mathrm{c}}$. To further compare the methods the interpolation between the S-N curves was excluded from the Volvo method, the results then showed a reduced deviation between methods.

Case 4 was set up such that the bending ratio could be adjusted with precision. The initial results further confirmed the expectations in an increased deviation between the methods for an increased bending ratio. To fully exclude the dependency of the empirically determined S-N curves, the interpolation between the S-N curves of the Volvo method was excluded. The remaining curve used was fitted to the S-N curve of the notch stress method for the case of full membrane loading. This resulted in equal life prediction for the two methods at full membrane loading for the tee joint. However, for an increased bending ratio the results showed an increased deviation in the life prediction. The deviation is due to the difference in stress extraction between the Volvo and notch stress method for an increased bending ratio. Assuming

that the notch stress method captures the stress variation between the load cases correctly, the results showed that the structural stress captured by the Volvo method is less conservative for bending dominated joints.

To compensate for the stress reduction of the Volvo method a function dependent on the bending ratio $h(\overline{\beta})$ could be introduced in the expression of the bending stress as

$$\sigma_{\perp}(y) = h(\overline{\beta}) \cdot \sigma_{\mathrm{b}}(y) + \sigma_{\mathrm{n}}(y) = -h(\overline{\beta}) \cdot \frac{12 m_{\mathrm{y}}(y) z}{t^3} - \frac{f_{\mathrm{x}}(y)}{t} \tag{5.1}$$

Another solution is the use of two S-N curves as already implemented in the Volvo method. The existing curve for bending dominated joints is however further increasing the deviation. No conclusion can be made on the validity of the bending dominated S-N curve in this thesis, physical tests are required. However, current research indicates that the fatigue strength increases for bending dominated loading [35]–[38]. A possible reason for the difference between the loading modes could be the different crack shape evolution related to the time to reach crack coalescence [37]. It should also be mentioned that a varying crack path dependent on $\overline{\beta}$ related to the varying ϕ_{p} has been identified, hence superposition for combined loading should be avoid [38].

With the material data used in the study it can be seen that the Volvo method was less conservative for the joints studied. Since no experimental correlation for the fatigue analysis has been done, further investigation is needed to validate the results. In general, a large spread in the experimental data is common when dealing with fatigue in welds. To get an understanding of the general behaviour, testing needs to be done with adequate documentation with a sufficient number of joint configurations and test samples.

For the Volvo method the fatigue life was extracted at half the width of the joint. From the FE results a variation in predicted life was observed over the width which was not considered. The difference was within 64%. Another error that has an influence on the results is the use of element stresses instead of the nodal value. The mesh of the notch stress model was refined to reduce the error but the fatigue life will always be overestimated with a stress error around 1.7%. While dealing with numerical solvers truncation errors can affect the results. In this study the influence was negligible compared to the above-mentioned sources of error. The largest source of uncertainty originates from the material data used for the Volvo method. Since the result could be discussed independent of the material data the uncertainty was accepted.

6
Conclusion

A direct comparison between the fatigue life predictions of the Volvo and notch stress method is not feasible since the behaviour is largely S-N curve dependent and the S-N curves are designed in different ways. The S-N curve of the notch stress method aims to provide conservative results for all applications with one master S-N curve at 97.7% survivability. The S-N curves of the Volvo method are designed to produce more nuanced results. This method differentiates the life depending on membrane versus bending stresses found in the experiments related to the method. For implementation of the methods, in-house fatigue testing is recommended to validate the fatigue properties.

- Both methods predicts similar fatigue life for $\overline{\beta} \leq \beta_c$ when the fatigue action is dominated by membrane stress.
- The deviation between the methods increases for increased $\overline{\beta}$ when the fatigue action is dominated by bending stress, $\overline{\beta} > \beta_c$.
- The stresses recovered from the Volvo method are not parallel to the stresses from the notch method for varying $\overline{\beta}$. This should be considered when implementing the method.

7
Future Work

In the thesis two ideal joints were studied. Further analysis with additional joints and loading conditions should be done to confirm the findings. The methods should also be compared for geometries with an increased complexity.

Since toe failure was the initial failure mode for the studied cases the comparison between the methods for root failure was not done. Additional investigations are recommended to find potential differences in the root life prediction. What could affect the fatigue life is the stiffness of the joint. Since the modelling technique differs between the two methods, studying the effect of varying throat size and weld angle would be interesting.

It was shown that the Volvo method was dependent on the bending ratio both for the fatigue resistance data and stress extraction. The notch stress method utilises one master S-N curve, but additional FAT classes dependent on bending ratio could be beneficial to predict a less conservative result. However, an investigation of the influence of the bending sensitivity compared to experimental data is needed for both methods.

As stated in the conclusion, testing is recommended to validate the results from the thesis. Load-life curves from experiments should be converted to S-N curves based on stress results from the corresponding FE models. While conducting the testing, thickness and mean stress correction should be considered.

Bibliography

[1] I. Al Zamzami and L. Susmel, "On the accuracy of nominal, structural, and local stress based approaches in designing aluminium welded joints against fatigue," *International Journal of Fatigue*, vol. 101, pp. 137–158, 2017. DOI: https://doi.org/10.1016/j.ijfatigue.2016.11.002.

[2] Z. Barsoum, "Guidelines for fatigue andstatic analysis of weldedand un-welded steelstructures," KTH Royal Institute of Technology, Stockholm, Sweden, Tech. Rep., 2020.

[3] N. E. Dowling, S. L. Kampe, and M. V. Kral, *Mechanical Behaviour of Materials*, 5th ed. Harlow, United Kingdom: Pearson Education Ltd., 2020.

[4] A. F. Hobbacher, *Recommendations for Fatigue Design of Welded Joints and Components*, 2nd ed. Cham, Switzerland: Springer Nature Switzerland AG, 2017. DOI: https://doi.org/10.1007/978-3-319-23757-2.

[5] *Eurocode 9: Design of aluminium structures - part 1-3: Structures susceptible to fatigue*, SS-EN 1999-1-3:2007, 2007.

[6] Å. Eriksson, A.-M. Lignell, C. Olsson, and H. Spennare, *Svetsutvärdering med FEM*, 1st ed. Stockholm, Sweden: Industrilitteratur AB, 2002.

[7] L. Susmel, "The modified wöhler curve method calibrated by using standard fatigue curves and applied in conjunction with the theory of critical distances to estimate fatigue lifetime of aluminium weldments," *International Journal of Fatigue*, vol. 31, no. 1, pp. 197–212, 2009. DOI: https://doi.org/10.1016/j.ijfatigue.2008.04.004.

[8] Z. Wei, J. Hamilton, F. Yang, L. Luo, and et al., "Comparison of verity and volvo methods for fatigue life assessment of welded structures," in *SAE 2013 Commercial Vehicle Engineering Congress*, 2013. DOI: https://doi.org/10.4271/2013-01-2357.

[9] J. Dakin, P. Heyes, M. Fermér, and D. Minen, "Analytical methods for durability in the automotive industry - the engineering process, past, present and future," in *SAE Brasil International Conference on Fatigue*, 2001. DOI: https://doi.org/10.4271/2001-01-4075.

[10] Python Software Foundation, *Python language reference*, version 3.9. Feb. 7, 2022. [Online]. Available: https://www.python.org/.

[11] Dassault Systèmes, *CATIA V5*, version 6R2019, Feb. 18, 2022. [Online]. Available: https://www.3ds.com/products-services/catia/.

[12] Beta CAE, *ANSA Pre-processor*, version 21.0.1. Mar. 14, 2022. [Online]. Available: https://www.beta-cae.com/ansa.htm.

[13] HyperWorks, *Altair OptiStruct™*, version 2021, Mar. 15, 2022. [Online]. Available: https://www.altair.com/optistruct/.

[14] Beta CAE, *META Post-processor*, version 21.0.1. Apr. 5, 2022. [Online]. Available: https://www.beta-cae.com/meta.htm.

[15] J.-L. Fayard, A. Bignonnet, and K. Dang Van, "Fatigue design of welded thin sheet structures," in *Fatigue Design of Components*, ser. European Structural Integrity Society, G. Marquis and J. Solin, Eds., vol. 22, Elsevier, 1997, pp. 145–152. DOI: https://doi.org/10.1016/S1566-1369(97)80015-5.

[16] M. Ericsson and R. Sandström, "Influence of welding speed on the fatigue of friction stir welds, and comparison with mig and tig," *International Journal of Fatigue*, vol. 25, no. 12, pp. 1379–1387, 2003. DOI: https://doi.org/10.1016/S0142-1123(03)00059-8.

[17] *Code of practice for fatigue design and assessment of steel structures*, BS7608, 1993.

[18] M. Fermér, M. Andréasson, and B. Frodin, "Fatigue life prediction of MAG-welded thin-sheet structures," in *International Body Engineering Conference & Exposition*, 1998. DOI: https://doi.org/10.4271/982311.

[19] C. Sonsino, W. Fricke, F. de Bruyne, A. Hoppe, A. Ahmadi, and G. Zhang, "Notch stress concepts for the fatigue assessment of welded joints – background and applications," *International Journal of Fatigue*, vol. 34, no. 1, pp. 2–16, 2012. DOI: https://doi.org/10.1016/j.ijfatigue.2010.04.011.

[20] Ö. Karakaş, J. Baumgartner, and L. Susmel, "On the use of a fictitious notch radius equal to 0.3 mm to design against fatigue welded joints made of wrought magnesium alloy az31," *International Journal of Fatigue*, vol. 139, p. 105 747, 2020. DOI: https://doi.org/10.1016/j.ijfatigue.2020.105747.

[21] J. Baumgartner, A. F. Hobbacher, and R. Rennert, "Fatigue assessment of welded thin sheets with the notch stress approach – proposal for recommendations," *International Journal of Fatigue*, vol. 140, p. 105 844, 2020. DOI: https://doi.org/10.1016/j.ijfatigue.2020.105844.

[22] D. Radaj, *Design and Analysis of Fatigue Resistant Welded Structures*, 1st ed. Cambridge, England: Woodhead Publishing, 1990. [Online]. Available: https://www.sciencedirect.com/book/9781855730045/design-and-analysis-of-fatigue-resistant-welded-structures.

[23] C. M. Sonsino, T. Bruder, and J. Baumgartner, "S-n lines for welded thin joints — suggested slopes and fat values for applying the notch stress concept

with various reference radii," *Welding in the World*, vol. 54, R375–R392, 2010. DOI: https://doi.org/10.1007/BF03266752.

[24] P. Heyes, J. Dakin, and C. St.John, "The assessment and use of linear static fe stress analyses for durability calculations," in *International Conference On Vehicle Structural Mechanics & Cae*, 1995. DOI: https://doi.org/10.4271/951101.

[25] Y.-L. Lee, M. E. Barkey, and H.-T. Kang, *Metal Fatigue Analysis Handbook : Practical Problem-Solving Techniques for Computer-aided Engineering*, 1st ed. Oxford, United States: Elsevier Science & Technology, 2012. DOI: https://doi.org/10.1016/C2010-0-66376-0.

[26] D. Radaj, C. M. Sonsino, and W. Fricke, *Fatigue assessment of welded joints by local approaches*, 2nd ed. Cornwall, England: Woodhead ublishing, 2006. [Online]. Available: https://www.sciencedirect.com/book/9781855739482/fatigue-assessment-of-welded-joints-by-local-approaches.

[27] Y. Liu, L. Zou, Y. Sun, and X. Yang, "Evaluation model of aluminum alloy welded joint low-cycle fatigue data based on information entropy," *Entropy*, vol. 19, no. 1, 2017. DOI: https://doi.org/10.3390/e19010037.

[28] P. Fransson and G. Pettersson, "Fatigue life prediction using forces in welded plates of moderate thickness," M.S. thesis, Blekinge Institute of Technology, Karlskrona, Sweden, 2000.

[29] M. Andréasson and B. Frodin, "Fatigue life prediction of MAG-welded thin sheet structures: Theory and experiments," M.S. thesis, Chalmers University of Technology, Gothenburg, Sweden, 1997.

[30] *HBM nCode: DesignLife™ Theory Guide*, HBM United Kingdom Ltd., Rotherham, United Kingdom, 2018.

[31] J. Baumgartner and T. Bruder, "An efficient meshing approach for the calculation of notch stresses," *Welding in the World*, vol. 57, pp. 137–145, 2013. DOI: https://doi.org/10.1007/s40194-012-0005-3.

[32] MSC Software, *NASTRAN*, version 2017.1.0. Apr. 8, 2022. [Online]. Available: https://www.mscsoftware.com/product/msc-nastran/.

[33] M. Fermér and H. Svensson, "Industrial experiences of fe-based fatigue life predictions of welded structures," *Fatigue & Fracture of Engineering Materials & Structures*, vol. 24, pp. 489–500, 2001. DOI: https://doi.org/10.1046/j.1460-2695.2001.00409.x.

[34] Z. Tahir, R. Aso, T. Yates, M. Bell, and A. Muse, "Aluminium weld fatigue: From characterisation to design rules," *Procedia Engineering*, vol. 213, pp. 549–570, 2018. DOI: https://doi.org/10.1016/j.proeng.2018.02.051.

[35] B. Baik, K. Yamada, and T. Ishikawa, "Fatigue strength of fillet welded joint subjected to plate bending," *International journal of steel structures*, vol. 8,

pp. 163–169, 2008. DOI: https://doi.org/10.1016/S0142-1123(01)00028-7.

[36] A. Ahola, T. Björk, and Z. Barsoum, "Fatigue strength capacity of load-carrying fillet welds on ultra-high-strength steel plates subjected to out-of-plane bending," *Engineering Structures*, vol. 196, p. 109 282, 2019. DOI: https://doi.org/10.1016/j.engstruct.2019.109282.

[37] Z. Mikulski and T. Lassen, "Crack growth in fillet welded steel joints subjected to membrane and bending loading modes," *Engineering Fracture Mechanics*, vol. 235, p. 107 190, 2020. DOI: https://doi.org/10.1016/j.engfracmech.2020.107190.

[38] A. Ahola, H. Rohani Raftar, T. Björk, and O. Kukkonen, "On the interaction of axial and bending loads in the weld root fatigue strength assessment of load-carrying cruciform joints," *Welding in the World*, vol. 66, pp. 731–744, 2022. DOI: https://doi.org/10.1007/s40194-021-01237-6.

DEPARTMENT OF SOME SUBJECT OR TECHNOLOGY
CHALMERS UNIVERSITY OF TECHNOLOGY
Gothenburg, Sweden
www.chalmers.se

CHALMERS
UNIVERSITY OF TECHNOLOGY